

Robust treatment of cross points in Optimized Schwarz Methods

X. Claeys¹ and E. Parolin²

¹Sorbonne Université, Université Paris-Diderot SPC, CNRS, Inria, Laboratoire
Jacques-Louis Lions, équipe Alpines, *claeys@ljl.math.upmc.fr*

²POems, UMR CNRS/ENSTA/Inria, Institut Polytechnique de Paris,
emile.parolin@inria.fr

Abstract

In the field of Domain Decomposition (DD), Optimized Schwarz Method (OSM) appears to be one of the prominent techniques to solve large scale time-harmonic wave propagation problems. It is based on appropriate transmission conditions using carefully designed impedance operators to exchange information between sub-domains. The efficiency of such methods is however hindered by the presence of cross-points, where more than two sub-domains abut, if no appropriate treatment is provided.

In this work, we propose a new treatment of the cross-point issue for the Helmholtz equation that remains valid in any geometrical interface configuration. We exploit the multi-trace formalism to define a new exchange operator with suitable continuity and isometry properties. We then develop a complete theoretical framework that generalizes classical OSM to partitions with cross points and contains a rigorous proof of geometric convergence, uniform with respect to the mesh discretization, for appropriate positive impedance operators. Extensive numerical results in 2D and 3D are provided as an illustration of the performance of the proposed method.

Introduction

Domain Decomposition (DD) for time-harmonic wave propagation is presently an active field of research as the numerical simulation of large scale problems remains a challenge in scientific computing. The additional difficulty of such problems, in comparison to elliptic problems, mainly lies in the (a priori) indefiniteness of the Helmholtz equation and related linear systems after discretization. In this work, we are interested in the sub-class of so-called (non-overlapping) Optimized Schwarz Methods (OSM) that appear as the most established approach in a wave context. In the context of waves, OSM dates back to the PhD thesis of Després [14, 15, 16, 17] where the idea to use Robin or impedance like transmission quantities was first introduced and a proof of algebraic convergence using energy estimates was derived. Many refinements over this initial idea were proposed since then in order to improve the rate of convergence exhibited. Most of the methods that were latter derived rely on the definition of a generalized Robin quantity with the introduction of an impedance operator. In this spirit, second order impedance operators (which possess sufficient properties for guaranteed convergence) were introduced by Gander, Magoulès and Nataf [21] and detailed in later

works [23, 29]. A popular approach was then developed which consists in using a (high-order) absorbing boundary condition (ABC) as transmission condition. The underlying idea is to approximate the Dirichlet-to-Neumann (DtN) map in the complementary domain, which provides exact transparent conditions albeit at a prohibitive numerical cost. This is the approach adopted in [4, 19] for instance where Padé-approximants of the square root operator are used to construct high-order ABC. However, despite their efficiency in practice, such methods lack a rigorous analysis of convergence since only partial proofs in specific geometries are available. Another alternative, advocated in [12, 13, 27], is to use suitable non-local operators, realized in practice with integral operators, as impedance operators. One of the strengths of this later approach is to rely on a solid theoretical basis that systematically guarantees (h -uniform [9]) geometric convergence, provided that certain properties of injectivity, surjectivity and positivity (in suitable trace spaces) are satisfied by the impedance operator.

For realistic large scale applications, DD methods should be applicable to domain partitions with cross points, where at least three sub-domains share a common vertex. The presence of such points can be an issue both for the analysis at the continuous level and in practice for numerical implementations. For DD methods used in conjunction with zeroth order transmission operators, the convergence proof is established at the continuous level and in the case of mixed finite elements discretizations, for instance in [16]. Interestingly, this particular choice of discretization avoids degrees of freedom (DOF) at cross points and therefore the issue altogether. In contrast, the junction issue arises if one makes the choice of using nodal finite element discretizations, see [28, 34]. Gander and Kwok [20] pointed out that straightforward nodal discretization of OSM can diverge and that the continuous proof (based on Lions' energy estimates) fails to carry over to the discrete setting in general. Some ad-hoc treatment of the problem at the discrete level have been developed which introduce additional global unknowns at the junction points effectively coupling all sub-domains [1, 2]. This lead to a global indefinite system that needs to be solved at each iteration. As regards the continuous theory available for DD methods constructed using non-local operators [12, 13, 27], it rests unfortunately on the strong hypothesis of the absence of cross-points between interfaces [27, Rem. 3]. Analysis suggests that this issue is related to the exchange operator being not continuous in proper trace norms in the presence of cross points. Recently, Modave *et al* [30] presented a treatment of cross points in the context of high-order ABC based transmission conditions. This later approach is however only valid on Cartesian like partitions of the mesh, allowing only cross points where exactly four domains abut (in 2D). It is clear that being able to deal with more general partitions, generated for instance by graph partitioners, is a highly desired property.

The goal of this work is to use the clean treatment of cross-points from the Multi-Trace (MTF) formalism [10], initially developed for boundary integral equations (BIE), to investigate OSM. The main idea is to introduce a regularized version of the exchange operator, that remains isometric and continuous regardless of cross points. The starting point is to recognize that if one uses positive impedance operators in the DD algorithm, it is possible to define a scalar product on the multi-trace space (collection of traces of local solutions in the sub-domains). We then use this scalar product to define an orthogonal projector onto the single-trace space (collection of traces that match across interfaces), which is a closed subspace of the multi-trace space, in a very natural way. This provides a discrete characterization of the continuity of both the Dirichlet and Neumann traces across interfaces, that remains valid in the presence of junctions. The definition of the exchange operator exploits this characterization using orthogonal projection and can be realized in practice by solving a positive linear system

posed on the skeleton of the partition. As a result, since its computation amounts to solving a linear system, the exchange operator is *a priori* non local. However, the structure of the auxiliary problem and in particular its definiteness are propitious to an efficient inversion, even in a distributed-memory parallelization context. Note that some closely related ideas have been developed in a previous work [8] by the first author, at the continuous level. In contrast to this work, the exchange operator was there defined explicitly in terms of boundary integral operators and the projector only defined implicitly.

Having defined this new way of exchanging traces across interfaces, the classical DD algorithms remain unchanged and the coupled local systems can be equivalently recast as a problem posed on the skeleton as usual. In fact, in the absence of cross points, one falls back on traditional OSM and one can see this work as a possible generalization of previously described methods. The continuity and isometric properties of the exchange operator together with the contractivity of the local scattering operators yields immediately geometric convergence of the Richardson algorithm, despite the presence of cross points. We show that in the case of geometric partitioning, using uniformly bounded impedance operators with respect to mesh discretization allows to get uniform convergence rate.

The present contribution describes what we believe is the first DDM substructuring strategy for waves with guaranteed geometric convergence regardless of the presence of cross points. We also provide a theoretical framework that applies in general geometric configurations while previous theoretical contributions on OSM either discarded the presence of cross points [12, 13, 27], proposed a convergence result with no estimate of the convergence rate [16], or considered positive definite problems [22, 28, 31]

This article is organized as follows. In Section 1 we shortly describe the problem under consideration, before describing the geometric partitioning in Section 2. The definitions of impedance operators and associated scalar products are then given in Section 3. In Section 4, the essential Lemma 4.3 states the properties of the exchange operator and the discrete characterization of the continuity of Dirichlet and Neumann traces. Section 5 recasts the problem at the interface and proves that the equivalent problem and the local subproblems are well posed for sufficiently small mesh parameter. Section 6 describes the usual Richardson algorithm of our DD method and Theorem 6.1 states that one obtains geometric convergence of the iterative solution towards the solution of the original model problem. Section 7 on discrete stability gives an explicit lower bound for the inf-sup constant associated to the problem on the skeleton. This result yields uniform rate of convergence of iterative algorithms with respect to the mesh discretization, in the particular case of uniformly bounded impedance operators, as stated in Section 8 in Corollary 8.2. We show how the proposed method is a generalization of classical OSM in Section 9. The algorithm in matrix form is detailed in Section 10, before extensive numerical results are reported in Section 11. We provide iteration counts for the Richardson and GMRES algorithms in 2D and 3D configurations with junction points with physical boundaries as well as interior cross points. The influence of several impedance operators with respect to different parameters: typical mesh size, wavenumber, number of sub-domains (strong and weak scalability) and varying coefficients (heterogeneous medium) is studied.

1 Problem under study

We consider a very classical boundary value problem modeling scalar wave propagation in an *a priori* heterogeneous medium in \mathbb{R}^d with $d = 1, 2$ or 3 . The computational domain $\Omega \subset \mathbb{R}^d$ will be assumed to be bounded and polygonal ($d = 2$) or polyhedral ($d = 3$) for the sake of simplicity. The material characteristics of the propagation medium will be represented by two measurable functions satisfying the following assumptions.

Assumption 1.

The functions $\kappa : \Omega \rightarrow \mathbb{C}$ and $\mu : \Omega \rightarrow (0, +\infty)$ satisfy

- (i) $\sup_{\mathbf{x} \in \Omega} |\kappa(\mathbf{x})| < +\infty$, and $\Im\{\kappa(\mathbf{x})\} \geq 0$, $\Re\{\kappa(\mathbf{x})\} \geq 0 \forall \mathbf{x} \in \Omega$
- (ii) $\sup_{\mathbf{x} \in \Omega} |\mu(\mathbf{x})| + |\mu^{-1}(\mathbf{x})| < +\infty$.

These are both general and physically reasonable assumptions. Condition (i) above implies in particular that $\Im\{\kappa^2(\mathbf{x})\} \geq 0$ and $\Im\{\iota\kappa(\mathbf{x})\} \geq 0$ for all $\mathbf{x} \in \Omega$. It means that the medium can only absorb or propagate energy. In addition, we consider source terms $f \in L^2(\Omega)$ and $g \in L^2(\partial\Omega)$. The boundary value problem under consideration will be

$$\begin{cases} \text{Find } u \in H^1(\Omega) \text{ such that} \\ \operatorname{div}(\mu \nabla u) + \kappa^2 u = -f \quad \text{in } \Omega, \\ (\mu \partial_{\mathbf{n}} - \iota \kappa) u = g \quad \text{on } \partial\Omega. \end{cases} \quad (1)$$

where \mathbf{n} refers to the outward unit normal vector to $\partial\Omega$. As usual, for any domain $\omega \subset \mathbb{R}^d$, the space $H^1(\omega)$ refers to those $v \in L^2(\omega)$ such that $\nabla v \in L^2(\omega)$, equipped with the norm $\|v\|_{H^1(\omega)}^2 := \|v\|_{L^2(\omega)}^2 + \|\nabla v\|_{L^2(\omega)}^2$. We shall also need to consider Dirichlet trace space $H^{1/2}(\partial\omega) := \{v|_{\partial\omega}, v \in H^1(\omega)\}$ equipped with the norm $\|p\|_{H^{1/2}(\partial\omega)} := \inf\{\|v\|_{H^1(\omega)}, v|_{\partial\omega} = p\}$ which satisfies $\|v|_{\partial\omega}\|_{H^{1/2}(\partial\omega)} \leq \|v\|_{H^1(\omega)} \forall v \in H^1(\omega)$. As usual, Problem (1) can be put in variational form: Find $u \in H^1(\Omega)$ such that $a(u, v) = \ell(v) \forall v \in H^1(\Omega)$ where

$$\begin{aligned} a(u, v) &:= \int_{\Omega} \mu \nabla u \cdot \nabla \bar{v} - \kappa^2 u \bar{v} d\mathbf{x} - \iota \int_{\partial\Omega} \kappa u \bar{v} d\sigma \\ \ell(v) &:= \int_{\Omega} f \bar{v} d\mathbf{x} + \int_{\partial\Omega} g \bar{v} d\sigma \end{aligned}$$

We make the general assumption that the material characteristics guarantee unique solvability of the above boundary value problem.

Assumption 2.

Problem (1) admits a unique solution.

We are particularly interested in an effective numerical solution to (1), so we assume given a regular simplicial triangulation $\mathcal{T}_h(\Omega)$ of the domain Ω , and we assume it to be conforming $\bar{\Omega} = \cup_{\tau \in \mathcal{T}_h(\Omega)} \bar{\tau}$. Further we assume h -uniform shape regularity:

$$\liminf_{h \rightarrow 0, \tau \in \mathcal{T}_h(\Omega)} \sup\{\operatorname{diam}(B), B \text{ is a ball } \subset \tau\} / \operatorname{diam}(\tau) > 0 \quad (2)$$

We shall denote $V_h(\Omega) \subset H^1(\Omega)$ a space generated by conforming \mathbb{P}_k -Lagrange shape functions ($k \geq 1$) constructed on $\mathcal{T}_h(\Omega)$. If $\omega \subset \Omega$ is any open subset that is resolved by the triangulation

i.e. $\bar{\omega} = \cup_{\tau \in \mathcal{T}_h(\omega)} \bar{\tau}$, where $\mathcal{T}_h(\omega) \subset \mathcal{T}_h(\Omega)$, then we denote $V_h(\omega) := \{\varphi|_{\omega}, \varphi \in V_h(\Omega)\}$ and $V_h(\partial\omega) := \{\varphi|_{\partial\omega}, \varphi \in V_h(\Omega)\}$. We will focus on the discrete variational formulation

$$\begin{aligned} & \text{Find } u_h \in V_h(\Omega) \text{ such that} \\ & a(u_h, v_h) = \ell(v_h) \quad \forall v_h \in V_h(\Omega). \end{aligned} \quad (3)$$

Devising efficient domain decomposition algorithms to solve this discrete problem is the main goal of the present article. Despite indefiniteness of our wave propagation problem, it is a classical consequence of Lax-Milgram lemma and Cea's lemma (see e.g. [25, chap.2]) that unique solvability of Problem (1) implies unique solvability of (3) for a sufficiently fine mesh, and that the bilinear form $a(\cdot, \cdot)$ satisfies a uniform discrete inf-sup condition

$$\begin{aligned} \alpha_\star &:= \liminf_{h \rightarrow 0} \alpha_h > 0 \quad \text{where} \\ \alpha_h &:= \inf_{u \in V_h(\Omega) \setminus \{0\}} \sup_{v \in V_h(\Omega) \setminus \{0\}} \frac{|a(u, v)|}{\|u\|_{H^1(\Omega)} \|v\|_{H^1(\Omega)}}. \end{aligned} \quad (4)$$

2 Geometric partitioning

We wish to describe and analyse a particular strategy for the solution of Problem (3) based on domain decomposition. As a consequence we assume that the computational domain admits the decomposition

$$\begin{aligned} \bar{\Omega} &= \cup_{j=1}^J \bar{\Omega}_j^h, \quad \text{with } \Omega_j^h \cap \Omega_k^h = \emptyset \quad \text{for } j \neq k \\ \Sigma &:= \cup_{j=1}^J \Gamma_j^h, \quad \text{where } \Gamma_j^h := \partial\Omega_j^h, \end{aligned} \quad (5)$$

where each $\Omega_j^h \subset \Omega$ is itself a polyhedral domain that is exactly resolved by the triangulation. Figure 1 below gives examples of the type of triangulation we consider.

A typical situation occurs when the computational domain is decomposed as a first step in subdomains and, only afterwards, the mesh is generated in each subdomain separately. In this case, compatibility between subdomain triangulations has to be enforced at interfaces. An example of this situation is represented in Figure 1a. Each subdomain Ω_j^h , and the subdomain partition itself, then remains unchanged as $h \rightarrow 0$. This is the case when the following condition is satisfied.

Condition 3 (fixed partition).

The subdomains $\Omega_j^h = \Omega_j$, $j = 1, \dots, J$ are independent of the triangulation $\mathcal{T}_h(\Omega)$.

However, we will *not* consider that Condition 3 holds in general (except in the examples of Section 3 and in Section 8), because this partitioning approach is not the most convenient from a practical viewpoint. This is the reason why we refer to it as a ‘‘condition’’ instead of an ‘‘assumption’’.

Another approach consists in generating a mesh on the whole computational domain Ω first, and then subdividing it in subdomains by means of a graph partitioner such as e.g. METIS [26]. In this manner, conformity of subdomain triangulations at interfaces is automatically satisfied. However the partition itself has no reason to stabilize for $h \rightarrow 0$, and there is no guarantee that each subdomain geometrically converges. Boundaries of subdomains may get rougher as $h \rightarrow 0$. This second situation is depicted in Figure 1b.

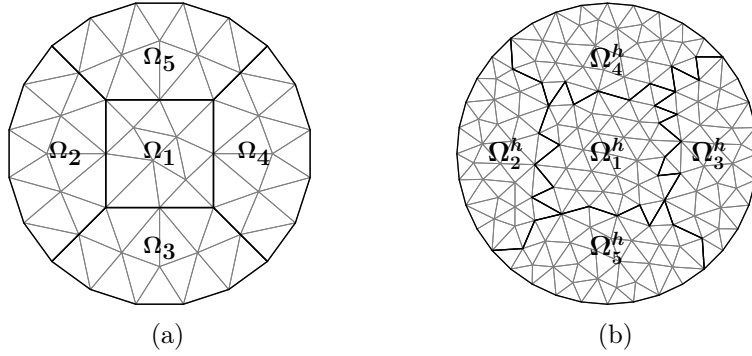


Figure 1: Two approaches for partitioning the computational domain.

The analysis we present here covers both situations (a) and (b). Our geometrical setting allows the presence of junctions on the skeleton Σ i.e. points where at least three subdomains may be adjacent. Because each Ω_j^h is resolved by the triangulation, so is each boundary Γ_j^h as well as the skeleton Σ . We introduce continuous and discrete function spaces naturally associated to this multi-domain setting $\mathbb{H}^1(\Omega) := \{u \in L^2(\Omega), u|_{\Omega_j^h} \in H^1(\Omega_j^h) \forall j = 1, \dots, J\}$ and

$$\mathbb{V}_h(\Omega) = \{u \in L^2(\Omega), u|_{\Omega_j^h} \in V_h(\Omega_j^h) \forall j = 1, \dots, J\} \subset \mathbb{H}^1(\Omega)$$

$$V_h(\Omega) := H^1(\Omega) \cap \mathbb{V}_h(\Omega)$$

The space $\mathbb{V}_h(\Omega)$ will be equipped with the norm $\|u\|_{\mathbb{H}^1(\Omega)}^2 := \|u\|_{H^1(\Omega_1^h)}^2 + \dots + \|u\|_{H^1(\Omega_J^h)}^2$. The elements of $\mathbb{V}_h(\Omega)$ may possibly admit Dirichlet jumps across interfaces between subdomains, while $V_h(\Omega)$ is a closed subspace of $\mathbb{V}_h(\Omega)$ characterized by the constraint that Dirichlet traces match across interfaces $\Gamma_j^h \cap \Gamma_k^h$. The sesquilinear form $a(\cdot, \cdot)$ extends as a map $a(\cdot, \cdot) : \mathbb{V}_h(\Omega) \times \mathbb{V}_h(\Omega) \rightarrow \mathbb{C}$ defined by

$$\begin{aligned} a(u, v) &:= \sum_{j=1}^J a_{\Omega_j^h}(u, v) \quad \text{where} \\ a_{\Omega_j^h}(u, v) &:= \int_{\Omega_j^h} \mu \nabla u \cdot \nabla \bar{v} - \kappa^2 u \bar{v} \, d\mathbf{x} - \iota \int_{\partial\Omega_j^h \cap \partial\Omega} \kappa u \bar{v} \, d\sigma \end{aligned}$$

Besides the inf-sup constant (4), the material characteristics μ, κ shall enter our forthcoming analysis through the continuity modulus

$$\|a\| := \sup_{u, v \in \mathbb{H}^1(\Omega) \setminus \{0\}} \frac{|a(u, v)|}{\|u\|_{\mathbb{H}^1(\Omega)} \|v\|_{\mathbb{H}^1(\Omega)}}$$

that is uniformly bounded by $\sup_{\Omega} (|\mu| + |\kappa|^2 + |\kappa|)$. Like for $a(\cdot, \cdot)$, the functional ℓ induces a continuous map on $\mathbb{V}_h(\Omega)$ defined by $\ell(v) = \sum_{j=1}^J \ell_{\Omega_j^h}(v)$ where $\ell_{\Omega_j^h}(v) := \int_{\Omega_j^h} f \bar{v} \, d\mathbf{x} + \int_{\partial\Omega_j^h \cap \partial\Omega} g \bar{v} \, d\sigma$ for all $v \in \mathbb{V}_h(\Omega)$. Since we will be interested in transmission conditions, we need to consider the trace operation

$$v|_{\Sigma} := (v|_{\Gamma_1^h}, \dots, v|_{\Gamma_J^h})$$

where each $v|_{\Gamma_j^h}$ is a Dirichlet trace taken from the interior of subdomain Ω_j^h , which is a convention we will systematically adopt through this article. The trace operator above continuously maps $\mathbb{V}_h(\Omega)$ onto the space of (Dirichlet) multi-traces

$$\mathbb{V}_h(\Sigma) := V_h(\Gamma_1^h) \times \dots \times V_h(\Gamma_J^h).$$

This space is naturally equipped with the norm associated to the cartesian product

$$\|\mathbf{u}\|_{\mathbb{H}^{1/2}(\Sigma)}^2 = \|u_1\|_{\mathbb{H}^{1/2}(\Gamma_1^h)}^2 + \cdots + \|u_J\|_{\mathbb{H}^{1/2}(\Gamma_J^h)}^2. \quad (6)$$

With this choice of norm, $\|v|_{\Sigma}\|_{\mathbb{H}^{1/2}(\Sigma)} \leq \|v\|_{\mathbb{H}^1(\Omega)}$ for all $v \in \mathbb{V}_h(\Omega)$ i.e. the trace operator is a contraction. There also exists a uniformly bounded lifting operator.

Proposition 2.1.

There exists a linear map $\rho_h : \mathbb{V}_h(\Sigma) \rightarrow \mathbb{V}_h(\Omega)$ such that $\rho_h(\mathbf{q})|_{\Sigma} = \mathbf{q} \forall \mathbf{q} \in \mathbb{V}_h(\Sigma)$ and that is uniformly bounded

$$\|\rho\| := \limsup_{h \rightarrow 0, \mathbf{q} \in \mathbb{V}_h(\Sigma) \setminus \{0\}} \frac{\|\rho_h(\mathbf{q})\|_{\mathbb{H}^1(\Omega)}}{\|\mathbf{q}\|_{\mathbb{H}^{1/2}(\Sigma)}} < +\infty.$$

Proof:

For each Ω_j^h for any $\mathbf{q} \in \mathbb{H}^1(\Gamma_j^h)$ let $\rho_j(\mathbf{q})$ refer to the unique element of $\mathbb{H}^1(\Omega_j^h)$ satisfying $\rho_j(\mathbf{q})|_{\Gamma_j^h} = \mathbf{q}$ and $\|\rho_j(\mathbf{q})\|_{\mathbb{H}^1(\Omega_j^h)} = \min\{\|v\|_{\mathbb{H}^1(\Omega_j^h)}, v \in \mathbb{H}^1(\Omega_j^h), v|_{\Gamma_j^h} = \mathbf{q}\}$. By definition $\|\rho_j(\mathbf{q})\|_{\mathbb{H}^1(\Omega_j^h)} = \|\mathbf{q}\|_{\mathbb{H}^{1/2}(\Gamma_j^h)}$. Next let $\pi_{h,j} : \mathbb{H}^1(\Omega_j^h) \rightarrow \mathbb{V}_h(\Omega_j^h)$ refer to the Scott-Zhang interpolation operator [33] and [5, §4.8]. This operator satisfies $\pi_{h,j}(v) = v$ for all $v \in \mathbb{V}_h(\Omega_j^h)$, and it is uniformly bounded

$$\limsup_{h \rightarrow 0} \|\pi_{h,j}(v)\|_{\mathbb{H}^1(\Omega_j^h)} / \|v\|_{\mathbb{H}^1(\Omega_j^h)} < +\infty$$

This modulus of the Scott-Zhang interpolator only depends on the shape regularity constant (2) of the triangulation and is thus bounded independently of the shape of the subdomains. Besides it can be defined in such a way that it guarantees $\pi_{j,h}(v)|_{\Gamma_j^h} = v|_{\Gamma_j^h}$ if $v|_{\Gamma_j^h} \in \mathbb{V}_h(\Gamma_j^h)$. Finally we define $\rho_h : \mathbb{V}_h(\Sigma) \rightarrow \mathbb{V}_h(\Omega)$ by setting

$$\rho_h(\mathbf{q}) := \sum_{j=1}^J 1_{\Omega_j^h}(\mathbf{x}) \pi_{j,h} \circ \rho_j(q_j)(\mathbf{x})$$

for all $\mathbf{q} = (q_1, \dots, q_J) \in \mathbb{V}_h(\Sigma)$. From the uniform continuity of $\rho_j, \pi_{j,h}, j = 1, \dots, J$ then follows the uniform continuity of ρ_h . \square

3 Impedance operator

To define a scalar product on the space of traces, one may of course consider the scalar product associated with (6). But many other choices are possible that appear more convenient in a finite element context. This is why we will *a priori* consider another one

$$t_h(\cdot, \cdot) : \mathbb{V}_h(\Sigma) \times \mathbb{V}_h(\Sigma) \rightarrow \mathbb{C} \text{ scalar product}$$

$$\|\mathfrak{w}\|_{\mathbb{V}_h(\Sigma)} := \sqrt{t_h(\mathfrak{w}, \mathfrak{w})}$$

that can be rather general. In particular we do not assume that $t_h(\cdot, \cdot)$ satisfies a uniform discrete inf-sup condition so that $\|\cdot\|_{\mathbb{V}_h(\Sigma)}$ need not be h -uniformly equivalent to $\|\cdot\|_{\mathbb{H}^{1/2}(\Sigma)}$. Hence, when discussing our discrete theory, the following two quantities shall play an important role

$$\lambda_h^- := \inf_{\mathfrak{w} \in \mathbb{V}_h(\Sigma) \setminus \{0\}} \frac{\|\mathfrak{w}\|_{\mathbb{V}_h(\Sigma)}}{\|\mathfrak{w}\|_{\mathbb{H}^{1/2}(\Sigma)}} \quad \lambda_h^+ := \sup_{\mathfrak{w} \in \mathbb{V}_h(\Sigma) \setminus \{0\}} \frac{\|\mathfrak{w}\|_{\mathbb{V}_h(\Sigma)}}{\|\mathfrak{w}\|_{\mathbb{H}^{1/2}(\Sigma)}} \quad (7)$$

Because $t_h(\cdot, \cdot)$ is supposed to be a scalar product, we have $0 < \lambda_h^- \leq \lambda_h^+ < +\infty$ for each h . However, in certain cases of practical importance, one may have $\liminf_{h \rightarrow 0} \lambda_h^- = 0$ or $\limsup_{h \rightarrow 0} \lambda_h^+ = +\infty$. To fix the ideas, we give a few examples of possible impedance operators.

Example 1 (Després impedance). Consider a fixed parameter $\kappa_R > 0$ that will serve as a reference mean wave number. A first possible choice consist in defining impedance using surface mass matrices as follows

$$t_h(\mathbf{p}, \mathbf{q}) = \sum_{j=1}^J \int_{\Gamma_j} \kappa_R p_j \bar{q}_j d\sigma \quad (8)$$

This choice of impedance was the one originally introduced in [14, 15, 16, 17]. It is a scalar product on $\mathbb{V}(\Sigma)$ that is h -uniformly bounded $\limsup_{h \rightarrow 0} \lambda_h^+ < +\infty$. If Condition 3 holds though, it does not satisfy any h -uniform discrete inf-sup condition. Inverse estimates show that there exists a constant $C > 0$ independent of h such that $\lambda_h^- \geq C\sqrt{h}$, see e.g [36, Lemma 4.11].

Example 2 (Second order differential operator). Consider two constants $a, b > 0$ that, in practice, are fitting parameters requiring calibration. Another choice of impedance is based on an order 2 surface differential operator and involves both mass and stiffness matrices

$$t_h(\mathbf{p}, \mathbf{q}) = \sum_{j=1}^J \int_{\Gamma_j} a \nabla_{\Gamma_j} p_j \cdot \nabla_{\Gamma_j} \bar{q}_j + b p_j \bar{q}_j d\sigma. \quad (9)$$

In the choice above, the operators ∇_{Γ_j} refer to surface gradients. Many variants of this condition can be considered. The coefficients a, b may vary from one subdomain to another i.e. $a = a_j$ (resp. $b = b_j$) on Γ_j . Also these coefficients may depend on the meshwidth h . Such a choice of impedance (or a variant of it) was considered e.g. in [21, 29, 23].

Impedance (9) also yields a scalar product on $\mathbb{V}_h(\Sigma)$. If Condition 3 holds, it can be proved to be h -uniformly inf-sup stable $\liminf_{h \rightarrow 0} \lambda_h^- > 0$, but it is not h -uniformly bounded anymore. Once again inverse estimates yield the existence of $C > 0$ independent of h such that $\lambda_h^+ \leq C/\sqrt{h}$.

Example 3 (Integral operator based impedance). Another possibility is an impedance based on some integral operator. Consider parameters $a, \delta > 0$. The parameter δ would represent how localized the kernel is. To mimic the properties of the trace norm, one may consider an analytical expression based on the hypersingular operator see e.g. [32, §3.3.4] or [35, §6.5]. For problems posed in \mathbb{R}^3 this would correspond to

$$t_h(\mathbf{p}, \mathbf{q}) = \sum_{j=1}^J \int_{\Gamma_j \times \Gamma_j} a \frac{\exp(-|\mathbf{x} - \mathbf{y}|/\delta)}{4\pi|\mathbf{x} - \mathbf{y}|} (\operatorname{curl}_{\Gamma_j} u(\mathbf{x}) \cdot \operatorname{curl}_{\Gamma_j} \bar{v}(\mathbf{y}) + \delta^{-2} \mathbf{n}_j(\mathbf{x}) \cdot \mathbf{n}_j(\mathbf{y}) u(\mathbf{x}) \bar{v}(\mathbf{y})) d\sigma(\mathbf{x}, \mathbf{y}) \quad (10)$$

where $\mathbf{n}_j(\mathbf{x})$ is the vector normal to Γ_j directed toward the exterior of Ω_j , and $\operatorname{curl}_{\Gamma_j} v(\mathbf{x}) := \mathbf{n}_j(\mathbf{x}) \times \nabla_{\Gamma_j} v(\mathbf{x})$ is the surface curl. Such a choice was considered in [13], and a variant of it was proposed in [11] in the context of Maxwell's equations.

Once again (10) is a scalar product on $\mathbb{V}_h(\Sigma)$. Because (10) stems from an operator that is both bounded and coercive in the continuous trace space, if Condition 3 holds, then $0 < \liminf_{h \rightarrow 0} \lambda_h^- \leq \limsup_{h \rightarrow 0} \lambda_h^+ < +\infty$.

In all the examples we gave above, the impedance does not couple distinct subdomains i.e. it takes the form of a sum of local contributions, which is rather natural in the context of domain decomposition.

Definition 3.1 (Diagonal impedance).

A scalar product $t_h(\cdot, \cdot) : \mathbb{V}_h(\Sigma) \times \mathbb{V}_h(\Sigma) \rightarrow \mathbb{C}$ will be called diagonal if there are local scalar products $t_h^j(\cdot, \cdot) : \mathbb{V}_h(\Gamma_j^h) \times \mathbb{V}_h(\Gamma_j^h) \rightarrow \mathbb{C}$ such that, for $\mathbf{p} = (p_1, \dots, p_J)$ and $\mathbf{q} = (q_1, \dots, q_J)$, we have

$$t_h(\mathbf{p}, \mathbf{q}) = t_h^1(p_1, q_1) + \dots + t_h^J(p_J, q_J).$$

Many other choices of impedance operator are possible, see e.g. [12, 27]. Much of the analysis we are presenting thereafter does not require the impedance to be diagonal. We shall comment later on the practical benefit of considering impedances of this form though.

To conclude this section we point out that the scalar product $t_h(\cdot, \cdot)$ will be used to represent linear functionals associated to boundary terms.

Lemma 3.2.

Assume that $\phi : \mathbb{V}_h(\Omega) \rightarrow \mathbb{C}$ is a linear form satisfying $\phi(w) = 0$ for all $w \in \mathbb{V}_h(\Omega)$ such that $w|_\Sigma = 0$. Then there exists a unique $\mathbf{q} \in \mathbb{V}_h(\Sigma)$ such that $\phi(v) = t_h(v|_\Sigma, \mathbf{q}) \forall v \in \mathbb{V}_h(\Omega)$.

Proof:

Since $w = \rho_h(v|_\Sigma) - v \in \mathbb{V}_h(\Omega)$ satisfies $w|_\Sigma = 0$ for all $v \in \mathbb{V}_h(\Omega)$, we deduce that $\phi(v) = \phi(\rho_h(v|_\Sigma))$ for all $v \in \mathbb{V}_h(\Omega)$. Since $t_h(\cdot, \cdot)$ is a scalar product on $\mathbb{V}_h(\Sigma)$, there exists a unique $\mathbf{q} \in \mathbb{V}_h(\Sigma)$ such that $t_h(\mathbf{p}, \mathbf{q}) = \phi(\rho_h(\mathbf{p})) \forall \mathbf{p} \in \mathbb{V}_h(\Sigma)$ by Riesz representation. \square

4 Characterization of interface conditions

In the present section, we will work out a convenient reformulation of our initial discrete problem (3). In this problem, Dirichlet transmission conditions are enforced by assuming that traces match across interfaces. To reformulate transmission conditions, it is thus natural to consider the subspace of tuples of traces that match across interfaces

$$\mathbb{V}_h(\Sigma) := \{(u|_{\Gamma_j^h})_{j=1}^J \in \mathbb{V}_h(\Sigma), u \in \mathbb{V}_h(\Omega)\}$$

This space is a discrete counterpart of what has been referred to as ‘‘Dirichlet single-trace’’ space in the literature dedicated to Multi-Trace formalism, see [6, 7, 10]. We first state a simple result that helps characterize $\mathbb{V}_h(\Omega)$ as a subspace of $\mathbb{V}_h(\Omega)$ by means of its traces on the skeleton.

Lemma 4.1.

Any $u \in \mathbb{V}_h(\Omega)$ belongs to $\mathbb{V}_h(\Omega)$ if and only if $u|_\Sigma \in \mathbb{V}_h(\Sigma)$.

An easy consequence of the previous lemma is that $\rho_h(\mathbf{q}) \in \mathbb{V}_h(\Omega)$ whenever $\mathbf{q} \in \mathbb{V}_h(\Sigma)$. The previous notations can be used to reformulate (3) as a saddle-point problem involving the space $\mathbb{V}_h(\Omega)$ instead of $\mathbb{V}_h(\Omega)$, and enforcing transmission conditions by means of Lagrange multipliers.

Proposition 4.2.

Denote $V_h(\Sigma)^\perp := \{\mathbf{u} \in \mathbb{V}_h(\Sigma), t_h(\mathbf{u}, \mathbf{v}) = 0 \forall \mathbf{v} \in V_h(\Sigma)\}$. If the function $u \in V_h(\Omega)$ solves (3), then there exists $\mathbf{q} \in V_h(\Sigma)^\perp$ such that

$$\begin{aligned} (u, \mathbf{q}) &\in \mathbb{V}_h(\Omega) \times V_h(\Sigma)^\perp \quad \text{and} \\ a(u, v) - t_h(\mathbf{q}, v|_\Sigma) &= \ell(v) \quad \forall v \in \mathbb{V}_h(\Omega), \\ t_h(u|_\Sigma, \mathbf{w}) &= 0 \quad \forall \mathbf{w} \in V_h(\Sigma)^\perp. \end{aligned} \tag{11}$$

Reciprocally if $(u, \mathbf{q}) \in \mathbb{V}_h(\Omega) \times V_h(\Sigma)^\perp$ solves (11), then $u \in V_h(\Omega)$ and it is the unique solution to Problem (3).

Proof:

Assume first that $u \in V_h(\Omega)$ solves (3). By definition we have $u|_\Sigma \in V_h(\Sigma)$ so that $t_h(u|_\Sigma, \mathbf{w}) = 0 \forall \mathbf{w} \in V_h(\Sigma)^\perp$. In addition, applying Lemma 3.2 to the functional $\phi(v) := a(u, v) - \ell(v), v \in \mathbb{V}_h(\Omega)$, we deduce that there exists $\mathbf{q} \in \mathbb{V}_h(\Sigma)$ such that $a(u, v) - \ell(v) = t_h(\mathbf{q}, v|_\Sigma) \forall v \in \mathbb{V}_h(\Omega)$. Besides we have $\phi(v) = 0 \forall v \in V_h(\Omega)$ by hypothesis which rewrites $t_h(\mathbf{q}, \mathbf{p}) = 0 \forall \mathbf{p} \in V_h(\Sigma)$ hence $\mathbf{q} \in V_h(\Sigma)^\perp$. This proves that (11) holds.

Reciprocally assume that (11) holds. According to Lemma 4.1, the second equation of (11) implies that $u \in V_h(\Omega)$. Next, taking $v \in V_h(\Omega)$ in the first equation (11) leads to $a(u, v) = \ell(v)$ for all $v \in V_h(\Omega)$, which is (3). In conclusion u solves (3). \square

Because we are aiming at domain decomposition, we wish to decouple subdomains as much as possible, and thus eliminate any reference to $V_h(\Sigma)$ in (11). This is our motivation in searching for characterizations of this space. The next result deals with this matter introducing an “exchange operator” Π . Its proof is routine verification left to the reader.

Lemma 4.3 (Exchange operator).

Assume that $\Pi : \mathbb{V}_h(\Sigma) \rightarrow \mathbb{V}_h(\Sigma)$ is such that $(\text{Id} + \Pi)/2$ is the orthogonal projector onto $V_h(\Sigma)$ for the scalar product t_h . Then Π is an isometry, we have $\Pi^2 = \text{Id}$ and $\|\Pi(\mathbf{u})\|_{\mathbb{V}_h(\Sigma)} = \|\mathbf{u}\|_{\mathbb{V}_h(\Sigma)}$ for all $\mathbf{u} \in \mathbb{V}_h(\Sigma)$. Moreover for any pair $(\mathbf{u}, \mathbf{q}) \in \mathbb{V}_h(\Sigma) \times \mathbb{V}_h(\Sigma)$ we have

$$(\mathbf{u}, \mathbf{q}) \in V_h(\Sigma) \times V_h(\Sigma)^\perp \iff -\mathbf{q} + \mathbf{u} = \Pi(\mathbf{q} + \mathbf{u}). \tag{12}$$

Computing the action of the exchange operator through the operation $\mathbf{p} \mapsto \Pi(\mathbf{p})$ is non-trivial from an effective computational viewpoint. This calculus can be achieved through an orthogonal projection onto the subspace $V_h(\Sigma)$ which, variationally, rewrites as follows

$$\begin{aligned} \Pi(\mathbf{q}) &:= -\mathbf{q} + 2\mathbf{p} \quad \text{where } \mathbf{p} \in V_h(\Sigma) \text{ solves} \\ t_h(\mathbf{p}, \mathbf{w}) &= t_h(\mathbf{q}, \mathbf{w}) \quad \forall \mathbf{w} \in V_h(\Sigma). \end{aligned} \tag{13}$$

Of course this orthogonal projection requires solving a problem posed globally on the whole skeleton Σ . Here the choice of the scalar product t_h does matter: it should be chosen so that the orthogonal projection in (13) is easy to compute. This variational problem makes the operator Π a priori non-local. For certain choices of impedance, this exchange operator may couple distant subdomain that are not a priori adjacent. This will be a salient feature of our strategy, and a key difference in comparison with existing literature.

Remark 1. Admittedly, this non-locality raises a computational difficulty. However the variational problem (13) is symmetric positive definite, and takes the very same form as the

Schur complement systems encountered in the analysis of substructuring methods, see [36, §4.3], [31, §2.1] or [18, §6.4]. Current literature offers very efficient scalable two level DDM preconditioners for tackling such a problem (13).

The exchange operator can be used to reformulate (11) in an advantageous way. Indeed (11) holds if and only if $(u, \mathbf{q}) \in \mathbb{V}_h(\Omega) \times \mathbb{V}_h(\Sigma)$ satisfies $a(u, v) - t_h(\mathbf{q}, v|_\Sigma) = \ell(v) \forall v \in \mathbb{V}_h(\Omega)$ and $(u|_\Sigma, \mathbf{q}) \in \mathbb{V}_h(\Sigma) \times \mathbb{V}_h(\Sigma)^\perp$. As a consequence (u, \mathbf{q}) solves (11) if and only if it satisfies

$$\begin{aligned} (u, \mathbf{q}) &\in \mathbb{V}_h(\Omega) \times \mathbb{V}_h(\Sigma) \quad \text{and} \\ a(u, v) - t_h(\mathbf{q}, v|_\Sigma) &= \ell(v) \quad \forall v \in \mathbb{V}_h(\Omega) \\ \mathbf{q} - u|_\Sigma &= -\Pi(\mathbf{q} + u|_\Sigma) \end{aligned} \tag{14}$$

When it is considered on $\mathbb{V}_h(\Omega) \times \mathbb{V}_h(\Sigma)$, the sesquilinear form $a(\cdot, \cdot)$ does not systematically satisfy an inf-sup condition. Resonance effects may appear in certain subdomains, which would be an artefact stemming from domain partitioning only. This is not satisfactory, and this is why we introduce a change of unknowns $\mathbf{p} = \mathbf{q} - u|_\Sigma \in \mathbb{V}_h(\Sigma)$ which leads to the new formulation

$$\begin{aligned} (u, \mathbf{p}) &\in \mathbb{V}_h(\Omega) \times \mathbb{V}_h(\Sigma) \quad \text{and} \\ (i) \quad a(u, v) - t_h(u|_\Sigma, v|_\Sigma) &= t_h(\mathbf{p}, v|_\Sigma) + \ell(v) \quad \forall v \in \mathbb{V}_h(\Omega) \\ (ii) \quad \mathbf{p} &= -\Pi(\mathbf{p} + 2u|_\Sigma) \end{aligned} \tag{15}$$

Due to the positivity properties of t_h , the sesquilinear form $u, v \mapsto a(u, v) - t_h(u|_\Sigma, v|_\Sigma)$ satisfies an inf-sup condition.

Lemma 4.4 (Well posedness of local subproblems).

There exists $h_0 > 0$ such that

$$\beta_h := \inf_{u \in \mathbb{V}_h(\Omega) \setminus \{0\}} \sup_{v \in \mathbb{V}_h(\Omega) \setminus \{0\}} \frac{|a(u, v) - t_h(u|_\Sigma, v|_\Sigma)|}{\|u\|_{\mathbb{H}^1(\Omega)} \|v\|_{\mathbb{H}^1(\Omega)}} > 0, \quad \forall h \in (0, h_0). \tag{16}$$

Proof:

Assume that the inf-sup constant above vanishes for some $h > 0$. This implies in particular that there exists $u \in \mathbb{V}_h(\Omega) \setminus \{0\}$ such that $a(u, v) - t_h(u|_\Sigma, v|_\Sigma) = 0 \forall v \in \mathbb{V}_h(\Omega)$. Since $\Im\{m\{\kappa^2\}\} \geq 0$ according to Assumption 1-(i) in Section 1, we have $0 = \int_\Omega \Im\{m\{\kappa(\mathbf{x})^2\}\} |u|^2 d\mathbf{x} + \int_{\partial\Omega} \Re\{\kappa\} |u|^2 d\sigma + t_h(u|_\Sigma, u|_\Sigma)$ hence $t_h(u|_\Sigma, u|_\Sigma) = 0 \Rightarrow u|_\Sigma = 0$. From this and Lemma 4.1, we conclude that $u \in \mathbb{V}_h(\Omega)$, and it satisfies $a(u, v) = a(u, v) - t_h(u|_\Sigma, v|_\Sigma) = 0$ for all $v \in \mathbb{V}_h(\Omega)$. This is not possible if $h \in (0, h_0)$ according to (4). \square

Whether or not the inf-sup stability pointed in the previous lemma holds uniformly in h is a legitimate question. Because our assumptions on $t_h(\cdot, \cdot)$ are rather loose though, it is difficult to discuss this at present stage. This uniform stability shall be examined when we discuss concrete choices of $t_h(\cdot, \cdot)$ later on.

5 Reduction to a problem on the skeleton

Well-posedness of subproblems allows introducing local scattering operators that eliminate volume unknowns, expressing \mathbf{p} in terms of u .

Lemma 5.1 (Scattering operator).

Let $S_h : \mathbb{V}_h(\Sigma) \rightarrow \mathbb{V}_h(\Sigma)$ refer to the continuous operator defined by $S_h(\mathbf{p}) = \mathbf{p} + 2w|_\Sigma$ where w is the unique element of $\mathbb{V}_h(\Omega)$ satisfying $a(w, v) - it_h(w|_\Sigma, v|_\Sigma) = t_h(\mathbf{p}, v|_\Sigma) \forall v \in \mathbb{V}_h(\Omega)$. Then we have $\|S_h(\mathbf{p})\|_{\mathbb{V}_h(\Sigma)} \leq \|\mathbf{p}\|_{\mathbb{V}_h(\Sigma)} \forall \mathbf{p} \in \mathbb{V}_h(\Sigma)$.

Proof:

From the definition of $w \in \mathbb{V}_h(\Omega)$ we deduce that $a(w, w) - it_h(w|_\Sigma, w|_\Sigma) = t_h(\mathbf{p}, w|_\Sigma)$. The properties of $a(\cdot, \cdot)$ then guarantee $\Im\{a(w, w)\} \leq 0$ which leads to the inequality $-\Re\{it_h(\mathbf{p}, w|_\Sigma)\} = \Im\{t_h(\mathbf{p}, w|_\Sigma)\} \leq -\|w|_\Sigma\|_{\mathbb{V}_h(\Sigma)}^2$. Next, developing the expression of the norm and using the previous inequality, we obtain $\|\mathbf{p} + 2w|_\Sigma\|_{\mathbb{V}_h(\Sigma)}^2 = \|\mathbf{p}\|_{\mathbb{V}_h(\Sigma)}^2 - 4\Re\{it_h(\mathbf{p}, w|_\Sigma)\} + 4\|w|_\Sigma\|_{\mathbb{V}_h(\Sigma)}^2 \leq \|\mathbf{p}\|_{\mathbb{V}_h(\Sigma)}^2$. \square

The contraction property that we have just established relates to energy conservation in each subdomain. We can use the scattering operator to write an equation posed only on the skeleton Σ as follows

$$\begin{aligned} \text{Find } \mathbf{p} \in \mathbb{V}_h(\Sigma) \text{ such that} \\ (\text{Id} + \Pi S_h)\mathbf{p} = \mathbf{f} \end{aligned} \tag{17}$$

where $\mathbf{f} := -2i\Pi(u_\star|_\Sigma)$ and $u_\star \in \mathbb{V}_h(\Omega)$ satisfies $a(u_\star, v) - it_h(u_\star|_\Sigma, v|_\Sigma) = \ell(v) \forall v \in \mathbb{V}_h(\Omega)$. Equation (17) is a reformulation of (15) as a problem posed on the skeleton Σ . Equation (17) is well posed.

Proposition 5.2 (Well posedness of transmission problem).

There exists $h_0 > 0$ such that $\text{Id} + \Pi S_h : \mathbb{V}_h(\Sigma) \rightarrow \mathbb{V}_h(\Sigma)$ is an isomorphism for all $h \in (0, h_0)$.

Proof:

We assume h_0 chosen as in Lemma 4.4. Since $\dim \mathbb{V}_h(\Sigma) < +\infty$ we only need to prove that $\ker(\text{Id} + \Pi S_h) = \{0\}$. Assume $\mathbf{p} \in \mathbb{V}_h(\Sigma)$ satisfies $(\text{Id} + \Pi S_h)\mathbf{p} = 0$. According to Lemma 4.4, there exists a unique $u \in \mathbb{V}_h(\Omega)$ solving $a(u, v) - it_h(u|_\Sigma, v|_\Sigma) = t_h(\mathbf{p}, v|_\Sigma) \forall v \in \mathbb{V}_h(\Sigma)$. Then the pair $(u, \mathbf{p}) \in \mathbb{V}_h(\Omega) \times \mathbb{V}_h(\Sigma)$ is solution to (15) with $\ell \equiv 0$. Since we have established equivalence between (15) and (3), see in particular Proposition 4.2, we conclude that u actually belongs to $\mathbb{V}_h(\Omega)$ and solves (3) with right-hand side $\ell \equiv 0$. Hence $u = 0$ according to (4) and thus $\mathbf{p} = 0$ since $t_h(\mathbf{p}, v|_\Sigma) = 0 \forall v \in \mathbb{V}_h(\Omega)$. \square

The operator $\text{Id} + \Pi S_h$ admits a special structure “*identity+contraction*”. This allows to prove its strong coercivity.

Corollary 5.3.

There exists $h_0 > 0$ such that, for all $h \in (0, h_0)$, we have

$$\begin{aligned} \Re\{t_h(\mathbf{p}, (\text{Id} + \Pi S_h)\mathbf{p})\} &\geq \frac{\gamma_h^2}{2} \|\mathbf{p}\|_{\mathbb{V}_h(\Sigma)}^2 \quad \forall \mathbf{p} \in \mathbb{V}_h(\Sigma) \\ \text{where } \gamma_h &:= \inf_{\mathbf{w} \in \mathbb{V}_h(\Sigma) \setminus \{0\}} \|(\text{Id} + \Pi S_h)\mathbf{w}\|_{\mathbb{V}_h(\Sigma)} / \|\mathbf{w}\|_{\mathbb{V}_h(\Sigma)} > 0. \end{aligned} \tag{18}$$

Proof:

Due to the contractivity properties given by the Lemmas 4.3 and 5.1, we have $\|\mathbf{p}\|_{\mathbb{V}_h(\Sigma)}^2 \geq \|\Pi S_h(\mathbf{p})\|_{\mathbb{V}_h(\Sigma)}^2 = \|((\text{Id} + \Pi S_h) - \text{Id})\mathbf{p}\|_{\mathbb{V}_h(\Sigma)}^2 = \|(\text{Id} + \Pi S_h)\mathbf{p}\|_{\mathbb{V}_h(\Sigma)}^2 + \|\mathbf{p}\|_{\mathbb{V}_h(\Sigma)}^2 - 2\Re\{t_h(\mathbf{p}, (\text{Id} + \Pi S_h)\mathbf{p})\}$. The result then comes when eliminating $\|\mathbf{p}\|_{\mathbb{V}_h(\Sigma)}^2$ from both sides of the inequality and using the definition of γ_h . \square

6 Convergent iterative algorithm

Usual iterative methods can be used to compute the solution to Problem (15) or one of the equivalent forms we have obtained for it. Here we examine the convergence of a Richardson's strategy: considering¹ a fixed relaxation parameter $r \in (0, 1)$, and starting from given initial data $u^{(0)}, \mathbf{p}^{(0)}$, we consider the algorithm

$$\begin{aligned} & (u^{(n)}, \mathbf{p}^{(n)}) \in \mathbb{V}_h(\Omega) \times \mathbb{V}_h(\Sigma) \text{ and} \\ & (i) \quad a(u^{(n)}, v) - \iota_h(u^{(n)}|_\Sigma, v|_\Sigma) = t_h(\mathbf{p}^{(n)}, v|_\Sigma) + \ell(v) \quad \forall v \in \mathbb{V}_h(\Omega) \\ & (ii) \quad \mathbf{p}^{(n)} = (1 - r)\mathbf{p}^{(n-1)} - r\Pi(\mathbf{p}^{(n-1)} + 2\iota u^{(n-1)}|_\Sigma) \end{aligned} \quad (19)$$

Each step of this algorithm involves two substeps. The multi-trace $\mathbf{p}^{(n)}$ should be computed first through (ii) which performs the exchange of information between subdomains, then $u^{(n)}$ should be computed (possibly in parallel) through (i).

Here it appears clearly why choosing diagonal impedance is interesting (cf Definition 3.1). Indeed in this case, the bilinear form appearing in (i) of (19) is itself diagonal $a(u, v) - \iota_h(u|_\Sigma, v|_\Sigma) = \sum_{j=1}^J a_{\Omega_j^h}(u, v) - \iota_h^j(u|_{\Gamma_j^h}, v|_{\Gamma_j^h})$. In this situation, solving (i) reduces to computing $u^{(n)} = (u_1^{(n)}, \dots, u_J^{(n)}) \in \mathbb{V}_h(\Omega)$ where

$$\begin{aligned} & u_j^{(n)} \in \mathbb{V}_h(\Omega_j^h) \text{ and} \\ & a_{\Omega_j^h}(u_j^{(n)}, v) - \iota_h^j(u_j^{(n)}|_{\Gamma_j^h}, v|_{\Gamma_j^h}) = t_h^j(p_j^{(n)}, v|_{\Gamma_j^h}) + \ell_{\Omega_j^h}(v) \quad \forall v \in \mathbb{V}_h(\Omega_j^h) \end{aligned} \quad (20)$$

where $\mathbf{p}^{(n)} = (p_1^{(n)}, \dots, p_J^{(n)})$. Such a problem must be solved for each $j = 1 \dots J$ independently. When the impedance is diagonal, solving such problems as (i) of (19) is then parallel. Without this feature though, Algorithm (19) seems pointless. This is why, from now on, we will make the additional assumption

Assumption 4.

The impedance $t_h(\cdot, \cdot)$ is diagonal, in the sense of Definition 3.1.

Assumption 4 has another important implication in a distributed-memory parallel implementation. Indeed, in this context a possible bottleneck is the cost of communication between processors.

The next result shows that the iterative scheme (19) converges toward the solution of our initial boundary value problem (3) with geometric convergence.

Theorem 6.1 (Geometric convergence of Richardson algorithm).

Let $\mathbf{p}^{(\infty)} \in \mathbb{V}_h(\Omega)$ refer to the unique solution to (17), consider the relaxation parameter $r \in (0, 1)$ and define γ_h as in (18). Then the iterates $\mathbf{p}^{(n)}$ computed by means of (19) satisfy the estimate

$$\frac{\|\mathbf{p}^{(n)} - \mathbf{p}^{(\infty)}\|_{\mathbb{V}_h(\Sigma)}}{\|\mathbf{p}^{(0)} - \mathbf{p}^{(\infty)}\|_{\mathbb{V}_h(\Sigma)}} \leq (1 - r(1 - r)\gamma_h^2)^{n/2}. \quad (21)$$

¹The choice of the relaxation parameter r follows heuristic considerations. If it is chosen to fit explicit calculus for the model geometric configuration of two domains and one spherical/circular interface, the value $r = 1/\sqrt{2}$ appears to be the optimal choice, see [11].

Proof:

The $\mathbf{p}^{(n)}$ defined through (19) satisfy the recurrence $\mathbf{p}^{(n)} = (1-r)\mathbf{p}^{(n-1)} - r\Pi S_h(\mathbf{p}^{(n-1)}) + \mathbf{f}$ with $\mathbf{f} \in \mathbb{V}_h(\Sigma)$ defined as in (17). We conclude that the sequence $\epsilon_n := \mathbf{p}^{(n)} - \mathbf{p}^{(\infty)}$ satisfies $\epsilon_n = (1-r)\epsilon_{n-1} - r\Pi S_h(\epsilon_{n-1})$. According to Lemma 4.3 and Lemma 5.1, we have $\|\Pi S_h(\mathbf{w})\|_{\mathbb{V}_h(\Sigma)} \leq \|\mathbf{w}\|_{\mathbb{V}_h(\Sigma)}$. From this we deduce

$$\begin{aligned} \|\epsilon_n\|_{\mathbb{V}_h(\Sigma)}^2 &= \|(1-r)\epsilon_{n-1} - r\Pi S_h(\epsilon_{n-1})\|_{\mathbb{V}_h(\Sigma)}^2 \\ &= (1-r)\|\epsilon_{n-1}\|_{\mathbb{V}_h(\Sigma)}^2 + r\|\Pi S_h(\epsilon_{n-1})\|_{\mathbb{V}_h(\Sigma)}^2 \\ &\quad - r(1-r)\|(\text{Id} + \Pi S_h)\epsilon_{n-1}\|_{\mathbb{V}_h(\Sigma)}^2 \\ &\leq (1-r(1-r)\gamma_h^2)\|\epsilon_{n-1}\|_{\mathbb{V}_h(\Sigma)}^2. \end{aligned}$$

□

Note that the constant $(1-r(1-r)\gamma_h^2)$ is positive, since $\gamma_h \leq 2$ from the Lemmas 4.3 and 5.1. Proposition 5.2 guarantees that $\gamma_h > 0$ in the previous result. This a priori does not discard the possibility that $\lim_{h \rightarrow 0} \gamma_h = 0$ and $\lim_{h \rightarrow 0} (1 - \gamma_h^2 r(1-r)) = 1$ which would correspond to a deterioration in the convergence of (19). On the other hand, if γ_h can be proved to remain bounded away from 0, this will correspond to h -uniform geometric convergence. Through the solution to local sub-problems, the previous theorem also yields a convergence estimate for $u^{(n)}$.

Corollary 6.2.

Let $(u^{(\infty)}, \mathbf{p}^{(\infty)})$ refer to the unique solution to (15), and suppose that the sequence $(u^{(n)}, \mathbf{p}^{(n)})$ has been defined through (19). Define γ_h as in (18), let β_h refer to the inf-sup constant of Lemma 4.4, and define λ_h^+ as in (7). Then we have the estimate

$$\frac{\|u^{(n)} - u^{(\infty)}\|_{\mathbb{H}^1(\Omega)}}{\|\mathbf{p}^{(0)} - \mathbf{p}^{(\infty)}\|_{\mathbb{V}_h(\Sigma)}} \leq \frac{\lambda_h^+}{\beta_h} (1-r(1-r)\gamma_h^2)^{n/2}.$$

Proof:

Set $e_n := u^{(n)} - u^{(\infty)}$ and $\epsilon_n := \mathbf{p}^{(n)} - \mathbf{p}^{(\infty)}$. Combining (19) with (15) we obtain that $a(e_n, v) - t_h(e_n|_{\Sigma}, v|_{\Sigma}) = t_h(\epsilon_n, v|_{\Sigma})$ for all $v \in \mathbb{V}_h(\Omega)$. We have $\|v|_{\Sigma}\|_{\mathbb{H}^{1/2}(\Sigma)} \leq \|v\|_{\mathbb{H}^1(\Omega)}$. Thus, using the inf-sup constant from Lemma 4.4, and the continuity modulus of t_h , we obtain $\beta_h \|e_n\|_{\mathbb{H}^1(\Omega)} \leq \lambda_h^+ \|\epsilon_n\|_{\mathbb{V}_h(\Sigma)}$. There only remains to apply Theorem 6.1. □

7 Discrete stability

The inf-sup constant (noted γ_h) of the operator $\text{Id} + \Pi S_h$ plays a crucial role in the bound for the convergence rate provided by Theorem 6.1. In the present section we analyse in more detail this quantity.

We first need to introduce $\mathbb{V}_h(\Sigma)^2 := \mathbb{V}_h(\Sigma) \times \mathbb{V}_h(\Sigma)$ equipped with the cartesian product norm $\|(\mathbf{p}, \mathbf{q})\|_{\mathbb{V}_h(\Sigma)^2} := (\|\mathbf{p}\|_{\mathbb{V}_h(\Sigma)}^2 + \|\mathbf{q}\|_{\mathbb{V}_h(\Sigma)}^2)^{1/2}$. We shall proceed by imitating the analytical approach presented in [8], which leads to introducing two subspaces

$$\begin{aligned} \mathcal{V}_h(\Sigma) &:= \mathbb{V}_h(\Sigma) \times \mathbb{V}_h(\Sigma)^\perp \\ \mathcal{C}_h(\Sigma) &:= \{ (\mathbf{u}_D, \mathbf{u}_N) \in \mathbb{V}_h(\Sigma)^2, \exists u \in \mathbb{V}_h(\Omega) \text{ such that } u|_{\Sigma} = \mathbf{u}_D \\ &\quad \text{and } a(u, v) = t_h(\mathbf{u}_N, v|_{\Sigma}) \forall v \in \mathbb{V}_h(\Omega) \} \end{aligned}$$

These are discrete counterparts of the single-trace and Cauchy data spaces considered in Section 4 and 6 of [8]. These are two complementary subspaces of the (discrete) multi-trace space.

Proposition 7.1.

We have $\mathbb{V}_h(\Sigma) \times \mathbb{V}_h(\Sigma) = \mathcal{V}_h(\Sigma) \oplus \mathcal{C}_h(\Sigma)$. Moreover, if $P_h : \mathbb{V}_h(\Sigma) \times \mathbb{V}_h(\Sigma) \rightarrow \mathcal{C}_h(\Sigma)$ is the projection onto $\mathcal{C}_h(\Sigma)$ with $\ker(P_h) = \mathcal{V}_h(\Sigma)$, then

$$\sup_{(\mathbf{p}, \mathbf{q}) \in \mathbb{V}_h(\Omega)^2 \setminus \{0\}} \frac{\|P_h(\mathbf{p}, \mathbf{q})\|_{\mathbb{V}_h(\Sigma)}^2}{\|(\mathbf{p}, \mathbf{q})\|_{\mathbb{V}_h(\Sigma)}^2} \leq \frac{(\lambda_h^+)^2 + (2\|a\| \cdot \|\rho\| / \lambda_h^-)^2}{\alpha_h}. \quad (22)$$

Proof:

Assume first that $(\mathbf{p}, \mathbf{q}) \in \mathcal{V}_h(\Sigma) \cap \mathcal{C}_h(\Sigma)$. Let $u \in \mathbb{V}_h(\Omega)$ satisfy $u|_\Sigma = \mathbf{p}$ and $a(u, v) = t_h(\mathbf{q}, v|_\Sigma) \forall v \in \mathbb{V}_h(\Omega)$. From $\mathbf{p} \in \mathbb{V}_h(\Sigma)$ and Lemma 4.1, we conclude that $u \in \mathbb{V}_h(\Omega)$, and since $\mathbf{q} \in \mathbb{V}_h(\Sigma)^\perp$, we have $a(u, v) = 0 \forall v \in \mathbb{V}_h(\Omega)$. Hence $u = 0$ according to (4), and thus $\mathbf{p} = \mathbf{q} = 0$. This proves that $\mathcal{V}_h(\Sigma) \cap \mathcal{C}_h(\Sigma) = \{0\}$.

Next we prove that $\mathbb{V}_h(\Sigma) \times \mathbb{V}_h(\Sigma) = \mathcal{V}_h(\Sigma) + \mathcal{C}_h(\Sigma)$. Pick $(\mathbf{p}, \mathbf{q}) \in \mathbb{V}_h(\Sigma) \times \mathbb{V}_h(\Sigma)$ arbitrarily, and define ψ as the unique solution to $\psi \in \mathbb{V}_h(\Omega)$ and $a(\psi + \rho_h(\mathbf{p}), v) = t_h(\mathbf{q}, v|_\Sigma) \forall v \in \mathbb{V}_h(\Omega)$. This function is bounded by

$$\|\psi\|_{\mathbb{H}^1(\Omega)} \leq \left(\frac{\|a\| \cdot \|\rho\|}{\alpha_h \lambda_h^-} \right) \|\mathbf{p}\|_{\mathbb{V}_h(\Sigma)} + \frac{\lambda_h^+}{\alpha_h} \|\mathbf{q}\|_{\mathbb{V}_h(\Sigma)} \quad (23)$$

Next rewriting $u := \psi + \rho_h(\mathbf{p})$, we set $\mathbf{u}_D := u|_\Sigma$. In addition, we have $a(u, w) = 0$ for all $w \in \mathbb{V}_h(\Omega)$ satisfying $w|_\Sigma = 0$ so, according to Lemma 3.2, we can define \mathbf{u}_N as the unique element of $\mathbb{V}_h(\Sigma)$ satisfying $t_h(\mathbf{u}_N, v|_\Sigma) = a(u, v) \forall v \in \mathbb{V}_h(\Omega)$ and actually $t_h(\mathbf{u}_N, \mathbf{w}) = a(u, \rho_h(\mathbf{w})) \forall \mathbf{w} \in \mathbb{V}_h(\Sigma)$. We deduce the estimates

$$\begin{aligned} \|u\|_{\mathbb{H}^1(\Omega)} &\leq \|\psi\|_{\mathbb{H}^1(\Omega)} + \frac{\|\rho\|}{\lambda_h^-} \|\mathbf{p}\|_{\mathbb{V}_h(\Sigma)} \\ \|\mathbf{u}_D\|_{\mathbb{V}_h(\Sigma)} &\leq \lambda_h^+ \|u\|_{\mathbb{H}^1(\Omega)} \\ \|\mathbf{u}_N\|_{\mathbb{V}_h(\Sigma)} &\leq \frac{\|a\| \cdot \|\rho\|}{\lambda_h^-} \|u\|_{\mathbb{H}^1(\Omega)} \end{aligned} \quad (24)$$

Now observe that $(\mathbf{u}_D, \mathbf{u}_N) \in \mathcal{C}_h(\Sigma)$ by construction. Besides we have $\mathbf{p} - \mathbf{u}_D = \rho_h(\mathbf{p})|_\Sigma - \mathbf{u}_D = -\psi|_\Sigma \in \mathbb{V}_h(\Sigma)$ since $\psi \in \mathbb{V}_h(\Omega)$. Finally we have $t_h(\mathbf{q} - \mathbf{u}_N, v|_\Sigma) = 0$ for all $v \in \mathbb{V}_h(\Omega)$ so that $\mathbf{q} - \mathbf{u}_N \in \mathbb{V}_h(\Sigma)^\perp$. We conclude that $(\mathbf{p}, \mathbf{q}) - (\mathbf{u}_D, \mathbf{u}_N) \in \mathcal{V}_h(\Sigma)$ and thus $(\mathbf{u}_D, \mathbf{u}_N) = P_h(\mathbf{p}, \mathbf{q})$. Finally Estimate (22) is obtained by combining (23) with (24) and observing that $\|a\|/\alpha_h \geq 1$ systematically. \square

Next we point that $\mathcal{C}_h(\Sigma)$ is closely related to the graph of the scattering operator S_h , as confirmed by the next lemma.

Lemma 7.2.

$\mathcal{C}_h(\Sigma) = \{(\mathbf{u}_D, \mathbf{u}_N) \in \mathbb{V}_h(\Sigma) \times \mathbb{V}_h(\Sigma), \mathbf{u}_N + \mathbf{u}_D = S_h(\mathbf{u}_N - \mathbf{u}_D)\}$.

Proof:

Take any $(\mathbf{u}_D, \mathbf{u}_N) \in \mathcal{C}_h(\Sigma)$. By definition there exists $u \in \mathbb{V}_h(\Omega)$ such that $u|_\Sigma = \mathbf{u}_D$ and $a(u, v) = t_h(\mathbf{u}_N, v|_\Sigma)$ for all $v \in \mathbb{V}_h(\Omega)$. This implies $a(u, v) - \iota t_h(u|_\Sigma, v|_\Sigma) = t_h(\mathbf{u}_N - \mathbf{u}_D, v|_\Sigma) \forall v \in \mathbb{V}_h(\Omega)$. Hence we have $S_h(\mathbf{u}_N - \mathbf{u}_D) = \mathbf{u}_N - \mathbf{u}_D + 2\iota u|_\Sigma = \mathbf{u}_N + \mathbf{u}_D$ according to the definition of the scattering operator given by Lemma 5.1.

Reciprocally, assume that $(\mathbf{u}_D, \mathbf{u}_N) \in \mathbb{V}_h(\Sigma)$ satisfies $\mathbf{u}_N + \mathbf{u}_D = S_h(\mathbf{u}_N - \mathbf{u}_D)$. Defining u as the unique element of $\mathbb{V}_h(\Omega)$ solving $a(u, v) - \iota t_h(u|_\Sigma, v|_\Sigma) = t_h(\mathbf{u}_N - \mathbf{u}_D, v|_\Sigma)$, we have $\mathbf{u}_N + \mathbf{u}_D = \mathbf{u}_N - \mathbf{u}_D + 2\iota u|_\Sigma \Rightarrow \mathbf{u}_D = u|_\Sigma$. From this we also deduce $a(u, v) = t_h(\mathbf{u}_N, v|_\Sigma)$ for all $v \in \mathbb{V}_h(\Omega)$. Hence $(\mathbf{u}_D, \mathbf{u}_N) \in \mathcal{C}_h(\Sigma)$. \square

The projection we have defined in Proposition 7.1 leads to an explicit expression of the inverse operator $(\text{Id} + \Pi S_h)^{-1}$, which we can use to bound the corresponding inf-sup constant.

Proposition 7.3.

$$\gamma_h := \inf_{\mathbf{w} \in \mathbb{V}_h(\Sigma) \setminus \{0\}} \frac{\|(\text{Id} + \Pi S_h)\mathbf{w}\|_{\mathbb{V}_h(\Sigma)}}{\|\mathbf{w}\|_{\mathbb{V}_h(\Sigma)}} \geq \frac{\sqrt{2}\alpha_h}{(\lambda_h^+)^2 + (2\|a\| \|\rho\|/\lambda_h^-)^2}.$$

Proof:

Pick an arbitrary $\mathbf{f} \in \mathbb{V}_h(\Sigma)$ and set $\mathbf{p}_D = \iota(\text{Id} - \Pi)\mathbf{f}/4$, $\mathbf{p}_N = (\text{Id} + \Pi)\mathbf{f}/4$. Observe that, due to the orthogonality of the projectors $(\text{Id} \pm \Pi)/2$ (Lemma 4.3), we have $\|(\mathbf{p}_D, \mathbf{p}_N)\|_{\mathbb{V}_h(\Sigma)^2}^2 = \|\mathbf{p}_D\|_{\mathbb{V}_h(\Sigma)}^2 + \|\mathbf{p}_N\|_{\mathbb{V}_h(\Sigma)}^2 = \|\mathbf{f}\|_{\mathbb{V}_h(\Sigma)}^2/4$. Next, considering the projection introduced in Proposition 7.1, define $(\mathbf{u}_D, \mathbf{u}_N) := P_h(\mathbf{p}_D, \mathbf{p}_N) \in \mathcal{C}_h(\Sigma)$. By construction we have $\mathbf{u}_D - \mathbf{p}_D \in V_h(\Sigma)$ and $\mathbf{u}_N - \mathbf{p}_N \in V_h(\Sigma)^\perp$. Applying Lemma 4.3, we obtain

$$\begin{aligned} -(\mathbf{u}_N - \mathbf{p}_N) + \iota(\mathbf{u}_D - \mathbf{p}_D) &= \Pi((\mathbf{u}_N - \mathbf{p}_N) + \iota(\mathbf{u}_D - \mathbf{p}_D)) \\ \iff \mathbf{u}_N - \mathbf{u}_D + \Pi(\mathbf{u}_N + \mathbf{u}_D) &= (\text{Id} + \Pi)\mathbf{p}_N - \iota(\text{Id} - \Pi)\mathbf{p}_D \\ &= [(\text{Id} + \Pi)/2]^2 \mathbf{f} + [(\text{Id} - \Pi)/2]^2 \mathbf{f} \\ &= (\text{Id} + \Pi)\mathbf{f}/2 + (\text{Id} - \Pi)\mathbf{f}/2 = \mathbf{f} \end{aligned}$$

Applying Lemma 7.2, we conclude that $(\text{Id} + \Pi S_h)(\mathbf{u}_N - \mathbf{u}_D) = \mathbf{f}$ which rewrites $\mathbf{u}_N - \mathbf{u}_D = (\text{Id} + \Pi S_h)^{-1}\mathbf{f}$. Finally, using Proposition 7.1, we obtain the estimate

$$\begin{aligned} \|(\text{Id} + \Pi S_h)^{-1}\mathbf{f}\|_{\mathbb{V}_h(\Sigma)} &= \|\mathbf{u}_N - \mathbf{u}_D\|_{\mathbb{V}_h(\Sigma)} \\ &\leq \sqrt{2}\|(\mathbf{u}_D, \mathbf{u}_N)\|_{\mathbb{V}_h(\Sigma)^2} = \sqrt{2}\|P_h(\mathbf{p}_D, \mathbf{p}_N)\|_{\mathbb{V}_h(\Sigma)^2} \\ &\leq \frac{(\lambda_h^+)^2 + (2\|a\| \|\rho\|/\lambda_h^-)^2}{\sqrt{2}\alpha_h} \|\mathbf{f}\|_{\mathbb{V}_h(\Sigma)}. \end{aligned}$$

\square

Combining the previous result with Lemma 5.3 or Theorem 6.1 obviously yields an estimate for the convergence rate of linear iterative solvers. In particular, when the impedance is chosen as equivalent to the scalar product associated to $\|\cdot\|_{\mathbb{H}^{1/2}(\Sigma)}$, convergence is then uniform with respect to the discretization parameter.

Corollary 7.4.

Let $\mathbf{p}^{(\infty)} \in V_h(\Omega)$ refer to the unique solution to (17), consider the relaxation parameter $r \in (0, 1)$. Assume in addition that $0 < \lambda_\star^- := \liminf_{h \rightarrow 0} \lambda_h^-$ and $\lambda_\star^+ := \limsup_{h \rightarrow 0} \lambda_h^+ < +\infty$.

Then for any $0 < \gamma_\star < \liminf_{h \rightarrow 0} \gamma_h$ there exists $h_0 > 0$ such that the iterates $\mathbf{p}^{(n)}$ computed by means of (19) satisfy the estimate

$$\frac{\|\mathbf{p}^{(n)} - \mathbf{p}^{(\infty)}\|_{\mathbb{V}_h(\Sigma)}}{\|\mathbf{p}^{(0)} - \mathbf{p}^{(\infty)}\|_{\mathbb{V}_h(\Sigma)}} \leq (1 - r(1 - r)\gamma_\star^2)^{n/2} \quad \forall h \in (0, h_0), \forall n \geq 0. \quad (25)$$

8 Fixed geometric partitions

In the present section, to obtain explicit results, we assume that Condition 3 holds, which corresponds to situation of Picture 1a. This implies in particular that the number J of sub-domains remains bounded.

Lemma 8.1.

Assume that Condition 3 is satisfied and that $t_h(\mathbf{p}, \mathbf{p}) = t(\mathbf{p}, \mathbf{p}) \forall \mathbf{p} \in \mathbb{V}_h(\Sigma)$ for a continuous positive definite sesquilinear form $t(\cdot, \cdot) : \mathbb{H}^{1/2}(\Sigma) \times \mathbb{H}^{1/2}(\Sigma) \rightarrow \mathbb{C}$ that does not depend on h . Then the inf-sup constant β_h defined in (16) is asymptotically uniformly bounded from below: $\beta_\star = \liminf_{h \rightarrow 0} \beta_h > 0$.

Proof:

We proceed by contradiction, assuming that there exist sequences $h_n \rightarrow 0$ and $u_n \in \mathbb{V}_{h_n}(\Omega)$ satisfying $\|u_n\|_{\mathbb{H}^1(\Omega)} = 1$ and

$$\lim_{n \rightarrow \infty} \sup_{v \in \mathbb{H}^1(\Omega) \setminus \{0\}} |a(u_n, v) - it(u_n, v)| / \|v\|_{\mathbb{H}^1(\Omega)} = 0. \quad (26)$$

Extracting a subsequence if necessary, we may assume that u_n converges toward some $u_\infty \in \mathbb{H}^1(\Omega)$ weakly in $\mathbb{H}^1(\Omega)$ such that $0 = \lim_{n \rightarrow \infty} \|u_n - u_\infty\|_{L^2(\Omega)} = \lim_{n \rightarrow \infty} \|u_n - u_\infty\|_{L^2(\partial\Omega)}$. Take any $v \in \mathbb{H}^1(\Omega)$ and let $v_n \in \mathbb{V}_{h_n}(\Omega)$ refer to its best approximation in the discrete variational space i.e. $\|v - v_n\|_{\mathbb{H}^1(\Omega)} = \inf\{\|v - w\|_{\mathbb{H}^1(\Omega)}, w \in \mathbb{V}_{h_n}(\Omega)\}$. In particular we have $\|v - v_n\|_{\mathbb{H}^1(\Omega)} \rightarrow 0$. Weak convergence of (u_n) together with (26) implies $a(u_n, v_n) - it(u_n, v_n) \rightarrow 0 = a(u_\infty, v) - it(u_\infty, v)$. Since v was chosen arbitrarily in $\mathbb{H}^1(\Omega)$ we conclude that $u_\infty = 0$, which implies $\lim_{n \rightarrow \infty} \|u_n\|_{L^2(\Omega)} = 0$. We finally obtain $\|u_n\|_{\mathbb{H}^1(\Omega)}^2 \leq C \Re\{a(u_n, u_n)\} + C \Re\{\int_\Omega \kappa^2(\mathbf{x}) |u_n|^2 d\mathbf{x}\} + \|u_n\|_{L^2(\Omega)}^2$ where $C = \sup_\Omega |\mu^{-1}| < +\infty$ according to Assumption 1. Since $\Re\{a(u_n, u_n)\} \rightarrow 0$ according to (26) and $\|u_n\|_{L^2(\Omega)} \rightarrow 0$, we deduce that $\|u_n\|_{\mathbb{H}^1(\Omega)} \rightarrow 0$ which yields a contradiction. \square

From Lemma 8.1 and assuming in addition uniform boundedness of the impedance operator, we easily get h -uniform convergence for the Richardson algorithm (19).

Corollary 8.2 (h -uniform geometric convergence for the Richardson algorithm).

Let $(u^{(\infty)}, \mathbf{p}^{(\infty)})$ refer to the unique solution to (15), and suppose that the sequence $(u^{(n)}, \mathbf{p}^{(n)})$ has been defined through (19). Assume that Condition 3 is satisfied and that $0 < \lambda_\star^- := \liminf_{h \rightarrow 0} \lambda_h^-$ and $\lambda_\star^+ := \limsup_{h \rightarrow 0} \lambda_h^+ < +\infty$. Then $0 < \liminf_{h \rightarrow 0} \gamma_h$ and for any $0 < \gamma_\star < \liminf_{h \rightarrow 0} \gamma_h$ there exists $h_0 > 0$ such that

$$\frac{\|u^{(n)} - u^{(\infty)}\|_{\mathbb{H}^1(\Omega)}}{\|\mathbf{p}^{(0)} - \mathbf{p}^{(\infty)}\|_{\mathbb{V}_h(\Sigma)}} \leq \frac{\lambda_\star^+}{\beta_\star} (1 - r(1 - r)\gamma_\star^2)^{n/2} \quad \forall h \in (0, h_0), \forall n \geq 0. \quad (27)$$

Now let us examine how the estimates of the previous section apply for the concrete choice of impedance considered in Section 3.

Example 1. *In the case of a fixed geometric partition, Després impedance fits the assumptions of Lemma 8.1. In addition, we have $\lambda_h^- = \mathcal{O}(\sqrt{h})$ and $\limsup_{h \rightarrow 0} \lambda_h^+ < +\infty$, so that $\gamma_h \geq ch$ for a constant $c > 0$ independent of h according to Proposition 7.3. Hence, Algorithm (19) satisfies the following convergence estimate in this case*

$$\frac{\|\mathbf{p}^{(n)} - \mathbf{p}^{(\infty)}\|_{\mathbb{V}_h(\Sigma)}}{\|\mathbf{p}^{(0)} - \mathbf{p}^{(\infty)}\|_{\mathbb{V}_h(\Sigma)}} \leq (1 - cr(1-r)h)^{n/2} \quad (28)$$

and a similar estimate holds for $\|u^{(n)} - u^{(\infty)}\|_{\mathbb{H}^1(\Omega)}$ cf Corollary 6.2. Although convergence holds with Després transmission condition, our theory suggests a deterioration in the convergence rate for $h \rightarrow 0$, and this deterioration is clearly visible on numerical examples, for instance in Figure 5a.

Example 2. *With a fixed geometric partition and impedance condition of second order (9), we can no longer guarantee uniform discrete inf-sup stability of local subproblems. In this case $\liminf_{h \rightarrow 0} \lambda_h^- > 0$ and $\limsup_{h \rightarrow 0} \lambda_h^+ = \mathcal{O}(1/\sqrt{h})$ so that, as in the previous example, $\gamma_h \geq ch$ for a constant $c > 0$ independent of h , and (28) holds. Once again we observe the deterioration in our numerical tests, for instance in Figure 5a. Unlike the preceding example, we do not have uniform discrete inf-sup stability, hence one cannot claim that $\|u^{(n)} - u^{(\infty)}\|_{\mathbb{H}^1(\Omega)}$ satisfy an estimate similar to (28).*

Example 3. *In the case of a fixed geometric partition, the impedance based on the hypersingular integral operator (10) fits the assumptions of Lemma 8.1 which yields uniform discrete local inf-sup stability. Besides we have $0 < \liminf_{h \rightarrow 0} \lambda_h^-$ and $\limsup_{h \rightarrow 0} \lambda_h^+ < +\infty$ so that $\gamma_\star = \liminf_{h \rightarrow 0} \gamma_h > 0$ and we have the h -uniform convergence estimate (25) of Corollary 7.4. It is remarkable that this convergence estimate does not depend on h . Uniform discrete local inf-sup stability then shows that the convergence estimate (27) holds for $\|u^{(n)} - u^{(\infty)}\|_{\mathbb{H}^1(\Omega)}$ according to Corollary 8.2.*

9 The case of no junction

The case where the subdomain partition (5) does not involve any junction is an important particular case, so we dedicate the present section to study this situation. The exchange operator Π becomes substantially simpler in this case. By “absence of junction point” we mean:

$$\begin{aligned} \Gamma_j^h \cap \Gamma_k^h \cap \Gamma_p^h &= \emptyset \quad \text{and} \\ \Gamma_j^h \cap \Gamma_k^h \cap \partial\Omega &= \emptyset \\ \text{for } j \neq k, k \neq p, p \neq j. \end{aligned} \quad (29)$$

We stress that this “no junction” assumption enforces two conditions: three subdomains cannot be adjacent at any point *and* two subdomains cannot meet at the physical boundary $\partial\Omega$ of the computational domain. Examples of such geometric configurations are given in Figure 2 below.

We wish to study this situation, so we assume all through this section that (29) holds. Then, each interface is a closed manifold. In this case, we can introduce an operator $X : \mathbb{V}_h(\Sigma) \rightarrow \mathbb{V}_h(\Sigma)$ consisting in swapping the traces from both sides of each interface

$$\mathbf{v} = X(\mathbf{w}) \iff \begin{cases} v_j = w_k & \text{on } \Gamma_j^h \cap \Gamma_k^h & j \neq k, \\ v_j = w_j & \text{on } \Gamma_j^h \cap \partial\Omega \end{cases} \quad (30)$$

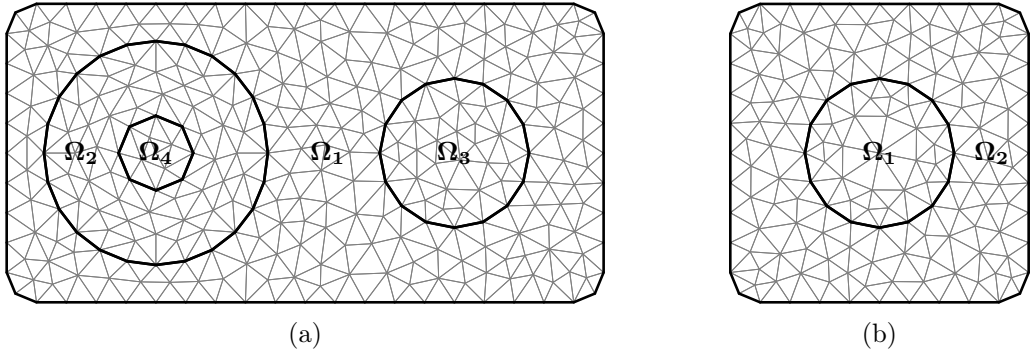


Figure 2: General partition with no junction (a) and partition with two domains only (b).

where $\mathbf{v} = (v_1, \dots, v_J)$, $\mathbf{w} = (w_1, \dots, w_J)$. This operator is widely spread in domain decomposition literature. It is in particular at the core of the Optimized Schwarz Methods (OSM), see [12, Formula (42)]. The next lemma (simple proof left to the reader) points a few elementary properties for this operator.

Lemma 9.1.

If (29) holds then the operator X defined by (30) maps continuously $\mathbb{V}_h(\Sigma)$ into $\mathbb{V}_h(\Sigma)$. Besides $X^2 = \text{Id}$ and $(\text{Id} + X)/2 : \mathbb{V}_h(\Sigma) \rightarrow \mathbb{V}_h(\Sigma)$ is a projector onto the single-trace space $\mathbb{V}_h(\Sigma)$.

There are striking similitudes shared by both Π and X , see the definition of Π given by Lemma 4.3. Both operators coincide, if and only if $(\text{Id} + X)/2$ is orthogonal for the scalar product $t_h(\cdot, \cdot)$, hence if and only if $(\text{Id} + X)/2$ is self-adjoint for the scalar product $t_h(\cdot, \cdot)$ which writes equivalently

$$t_h(X(\mathbf{v}), \mathbf{w}) = t_h(\mathbf{v}, X(\mathbf{w})) \quad \forall \mathbf{v}, \mathbf{w} \in \mathbb{V}_h(\Sigma). \quad (31)$$

This condition is satisfied only under certain conditions on the impedance $t_h(\cdot, \cdot)$. The next result provides sufficient conditions for this: roughly speaking the impedance operator should be “symmetric” with respect to all interfaces (except the physical boundary).

Proposition 9.2.

Assume that the impedance t_h is diagonal (cf Definition 3.1) and Condition (29) holds. Set $\mathcal{J} := \{(j, k) \in \{1, \dots, J\}^2, j < k \text{ and } \Gamma_j^h \cap \Gamma_k^h \neq \emptyset\}$ and $\Gamma_0^h := \partial\Omega$. Then $X = \Pi$ if there exist scalar products $t_h^{j,k} : \mathbb{V}_h(\Gamma_j^h \cap \Gamma_k^h) \times \mathbb{V}_h(\Gamma_j^h \cap \Gamma_k^h) \rightarrow \mathbb{C}$ such that

$$t_h(\mathbf{v}, \mathbf{w}) = \sum_{k \in \{1, \dots, J\}} t_h^{0,k}(v_k, w_k) + \sum_{(j,k) \in \mathcal{J}} (t_h^{j,k}(v_j, w_j) + t_h^{j,k}(v_k, w_k)) \\ \forall \mathbf{v} = (v_1, \dots, v_J), \quad \mathbf{w} = (w_1, \dots, w_J) \in \mathbb{V}_h(\Sigma).$$

Proof:

From (30), for $\mathbf{v} = (v_1, \dots, v_J)$ and $\mathbf{w} = (w_1, \dots, w_J)$ in $\mathbb{V}_h(\Sigma)$, we obtain the expression $t_h(X(\mathbf{v}), \mathbf{w}) = \sum_{k \in \{1, \dots, J\}} t_h^{0,k}(v_k, w_k) + \sum_{(j,k) \in \mathcal{J}} [t_h^{j,k}(v_j, w_k) + t_h^{j,k}(v_k, w_j)]$. This proves (31) which, as previously discussed, shows that $\Pi = X$. \square

The previous result states that, when there is no junction and the impedance does not couple disjoint interfaces (which is actually a natural choice of impedance), then $\Pi = X$. In this

situation, Algorithm (19) appears to be a classical Optimized Schwarz Method: this is exactly the algorithm appearing for example in [16, §3.3], [14], [21, §5] or [27, chap.6].

This shows that (19) is a true generalization of OSM for the case where the subdomain partition contains cross points.

10 Matrix form of the algorithm

Coming back to the general situation where the subdomain partition may admit junction points, in this section we will describe in more concrete terms the implementation of the iterative scheme (19), writing all equations in matrix form. This will help gaining a real insight on the implementation details underlying the solution strategy we propose.

First of all, we set a few matrix notations. We assume that the classical shape functions of \mathbb{P}_k -Lagrange finite elements are used, and we consider a numbering of the associated degrees of freedom in each subdomain and on each boundary: for $\Upsilon = \Omega_j^h$ or $\Upsilon = \Gamma_j^h$ for some $j = 1, \dots, J$ we define

$$N(\Upsilon) := \dim V_h(\Upsilon) \quad \text{and} \\ V_h(\Upsilon) = \text{span}_{k=1 \dots N_\Upsilon} \{\varphi_k^\Upsilon\}.$$

Here the φ_k^Υ 's refer to the usual \mathbb{P}_k -Lagrange shape functions associated to the triangulation in Υ . We assume that each shape function on Γ_j^h is obtained by taking the trace of some shape function on Ω_j^h . We also introduce local stiffness matrices \mathbf{A}_j with size $N(\Omega_j^h) \times N(\Omega_j^h)$, local impedance matrices \mathbf{T}_j with size $N(\Gamma_j^h) \times N(\Gamma_j^h)$, and local trace matrices \mathbf{B}_j with size $N(\Gamma_j^h) \times N(\Omega_j^h)$. The entries of these matrices are defined by

$$\begin{cases} (\mathbf{A}_j)_{k,l} := a_{\Omega_j^h}(\varphi_l^{\Omega_j^h}, \varphi_k^{\Omega_j^h}), \\ (\mathbf{T}_j)_{k,l} := t_h^j(\varphi_l^{\Gamma_j^h}, \varphi_k^{\Gamma_j^h}), \end{cases} \quad \begin{cases} (\mathbf{B}_j)_{k,l} := 1 & \text{if } \varphi_k^{\Gamma_j^h} = \varphi_l^{\Omega_j^h}|_{\Gamma_j^h}, \\ (\mathbf{B}_j)_{k,l} := 0 & \text{otherwise.} \end{cases}$$

Finally we also set $N(\Sigma) := \dim V_h(\Sigma)$. For each degree of freedom $k = 1, \dots, N(\Sigma)$, set $s(k, j) = 0$ if k does not belong to Γ_j^h , and let $s(k, j)$ refer to the number of this degree of freedom local to Γ_j^h otherwise. The assumptions of conformity we formulated on the triangulation (see Section 1 and 2) guarantee that we can find a basis of shape functions $V_h(\Sigma) = \text{span}_{k=1 \dots N_\Sigma} \{\varphi_k^\Sigma\}$ where

$$\varphi_k^\Sigma = (\varphi_{s(k,1)}^{\Gamma_1^h}, \dots, \varphi_{s(k,J)}^{\Gamma_J^h}) \\ \text{setting } \varphi_0^{\Gamma_j^h} \equiv 0 \quad \forall j.$$

To keep track of this, we introduce boolean matrices \mathbf{Q}_j of size $N(\Gamma_j^h) \times N(\Sigma)$ defined by $(\mathbf{Q}_j)_{k,l} = 1$ if $k = s(l, j)$, and $(\mathbf{Q}_j)_{k,l} = 0$ otherwise. These matrices can be used to assemble \mathbf{T}_Σ the Galerkin matrix of the impedance $t_h(\cdot, \cdot)$ restricted to $V_h(\Sigma)$. It is of size $N(\Sigma) \times N(\Sigma)$ and admits the expression

$$(\mathbf{T}_\Sigma)_{k,l} := t_h(\varphi_k^\Sigma, \varphi_l^\Sigma) \\ \mathbf{T}_\Sigma = \mathbf{Q}_1^* \mathbf{T}_1 \mathbf{Q}_1 + \dots + \mathbf{Q}_J^* \mathbf{T}_J \mathbf{Q}_J.$$

Finally we also need to introduce local contributions of the right-hand side represented by vectors \mathbf{f}_j of size $N(\Omega_j^h)$ defined by $(\mathbf{f}_j)_k := \ell_{\Omega_j^h}(\varphi_k^{\Omega_j^h})$. After assembly of the matrices introduced above, and a proper choice of the relaxation parameter r and maximum number of iterations n_{\max} , the iterative scheme (19) takes the form of Algorithm (1) below. The whole algorithm is then parallel except for the step appearing in Line 10 which ensures coupling between subdomains (see also Remark 1).

Algorithm 1

```

1: for  $j = 1, \dots, J$  do ▷ Initialisation
2:    $\mathbf{p}_j = 0$  ▷ size:  $N(\Gamma_j^h)$ 
3:    $\mathbf{u}_j = (\mathbf{A}_j - \iota \mathbf{B}_j^* \mathbf{T}_j \mathbf{B}_j)^{-1} \mathbf{f}_j$  ▷ Local solve (size:  $N(\Omega_j^h)$ )
4: end for
5: for  $n = 1, \dots, n_{\max}$  do
6:    $\mathbf{g} = 0$  ▷ size:  $N(\Sigma)$ 
7:   for  $j = 1, \dots, J$  do
8:      $\mathbf{g} = \mathbf{g} + \mathbf{Q}_j^* \mathbf{T}_j (\mathbf{p}_j + 2\iota \mathbf{B}_j \mathbf{u}_j)$  ▷ Local scattering
9:   end for
10:   $\mathbf{v} = \mathbf{T}_\Sigma^{-1} \mathbf{g}$  ▷ Global exchange
11:  for  $j = 1, \dots, J$  do
12:     $\mathbf{p}_j = \mathbf{p}_j + 2r(\iota \mathbf{B}_j \mathbf{u}_j - \mathbf{Q}_j \mathbf{v})$ 
13:     $\mathbf{u}_j = (\mathbf{A}_j - \iota \mathbf{B}_j^* \mathbf{T}_j \mathbf{B}_j)^{-1} (\mathbf{B}_j^* \mathbf{T}_j \mathbf{p}_j + \mathbf{f}_j)$  ▷ Local solve (size:  $N(\Omega_j^h)$ )
14:  end for
15: end for

```

While the theoretical analysis of the Richardson algorithm (19) allows to get some deep insight on the efficiency of the method, such an algorithm is rarely used in practice. Krylov methods are the preferred choice in real-life applications, in particular one will typically resort to the GMRES algorithm in our non-symmetric case. Importantly, (h -uniform) geometric convergence of the Richardson algorithm guarantees (h -uniform) geometric convergence of its GMRES counter-part, even the restarted version.

Although other choices are possible, we solve iteratively using GMRES the linear system given by (17) which features a multi-trace as unknown. To define the algorithm, it suffices to provide a definition for a right-hand-side and a matrix-vector product routine. The right-hand-side is denoted by \mathbf{b} and can be computed (offline) according to Algorithm 2. The matrix-vector product procedure, which takes as input a vector \mathbf{p} and outputs a vector \mathbf{q} , is given in Algorithm 3. Notice again here that apart from the computation in Line 8 of Algorithm 3 which ensures coupling between subdomains, all operations are local to the subdomains (see also Remark 1).

Algorithm 2

1: $\mathbf{b} = 0$ ▷ size: $N(\Sigma)$
2: $\mathbf{g} = 0$ ▷ size: $N(\Sigma)$
3: **for** $j = 1, \dots, J$ **do**
4: $\mathbf{u}_j = (\mathbf{A}_j - \imath \mathbf{B}_j^* \mathbf{T}_j \mathbf{B}_j)^{-1} \mathbf{f}_j$ ▷ Local solve (size: $N(\Omega_j^h)$)
5: $\mathbf{b} = \mathbf{b} + 2\imath \mathbf{Q}_j^* \mathbf{B}_j \mathbf{u}_j$
6: $\mathbf{g} = \mathbf{g} + 2\imath \mathbf{Q}_j^* \mathbf{T}_j \mathbf{B}_j \mathbf{u}_j$
7: **end for**
8: $\mathbf{b} = \mathbf{b} - 2\mathbf{T}_\Sigma^{-1} \mathbf{g}$ ▷ Global exchange

Algorithm 3

1: $\mathbf{q} = 0$ ▷ size: $N(\Sigma)$
2: $\mathbf{g} = 0$ ▷ size: $N(\Sigma)$
3: **for** $j = 1, \dots, J$ **do**
4: $\mathbf{u}_j = (\mathbf{A}_j - \imath \mathbf{B}_j^* \mathbf{T}_j \mathbf{B}_j)^{-1} (\mathbf{B}_j^* \mathbf{T}_j \mathbf{Q}_j \mathbf{p})$ ▷ Local solve (size: $N(\Omega_j^h)$)
5: $\mathbf{q} = \mathbf{q} - 2\imath \mathbf{Q}_j^* \mathbf{B}_j \mathbf{u}_j$
6: $\mathbf{g} = \mathbf{g} + \mathbf{Q}_j^* \mathbf{T}_j (\mathbf{Q}_j \mathbf{p} + 2\imath \mathbf{B}_j \mathbf{u}_j)$ ▷ Local scattering
7: **end for**
8: $\mathbf{q} = \mathbf{q} + 2\mathbf{T}_\Sigma^{-1} \mathbf{g}$ ▷ Global exchange

11 Numerics

In this section, we investigate numerically the performance of the above method. In all the numerical experiments given below, we solve the model Problem (1) in a domain Ω which is either a disk in 2D or a ball in 3D. Unless stated otherwise, we consider $\mu \equiv 1$ and the wavenumber κ is uniform in the domain. The source terms are taken to be $f \equiv 0$ and $g = (\mu \partial_{\mathbf{n}} - \imath \kappa) u_{\text{inc}}$ where $u_{\text{inc}}(\mathbf{x}) = e^{\imath \kappa \mathbf{d} \cdot \mathbf{x}}$ with \mathbf{d} the unit vector in the x direction.

We provide numerical results obtained for the Richardson algorithm (19) as well as results obtained with a restarted GMRES algorithm. In all our numerical experiments, the relaxation parameter of the Richardson algorithm is $r = 0.5$ and GMRES is restarted every 20 iterations.

We provide various tables reporting the number of iterations required to achieve a tolerance of 10^{-8} for the relative error defined at the iteration n as

$$(\text{relative error})^2 = \frac{\sum_{j=1 \dots J} \|u^{(n)} - u^{(\infty)}\|_{\mathbf{H}^1(\Omega_j^h)}^2}{\sum_{j=1 \dots J} \|u^{(0)} - u^{(\infty)}\|_{\mathbf{H}^1(\Omega_j^h)}^2}, \quad (32)$$

where $u^{(n)}$ is the volume solution at iteration n , $u^{(0)}$ is the initial volume solution (taken to be zero in practice) and $u^{(\infty)}$ is the exact discrete volume solution of the full (undecomposed) problem. The choice of this volume (energy) norm has the important benefit of being independent of the choice of impedance or mesh partition. Finally, we stress that the criterion for reaching convergence does not rely on the residual of the linear system that is solved. In all test runs that were performed, the convergence was stopped if a maximum number of 10^5 iterations was not enough to get to the set tolerance.

The impedance operators tested are: the Després impedance operator of Example 1, denoted by M with parameter $\kappa_R = \kappa$; the second order impedance operator of Example 2, denoted by K with parameters $a = \frac{1}{2\kappa}$ and $b = \kappa$; and the (hypersingular) boundary integral operator given in Example 3, denoted by W with parameters $a = \kappa^2$ and $\delta = \frac{1}{\kappa}$. In addition, we experimented with a DtN based impedance operator, denoted by Λ , which corresponds to the following scalar product:

$$t_h(\mathbf{p}, \mathbf{q}) = \sum_{j=1}^J \langle \mu \partial_{\mathbf{n}} v_j |_{\Gamma_j^h}, q_j \rangle_{\Gamma_j^h},$$

where $\mathbf{p} = (p_1, \dots, p_J)$, $\mathbf{q} = (q_1, \dots, q_J) \in \mathbb{V}_h(\Sigma)$ and $v_j \in H^1(\Omega_j^h)$ is the solution of the following coercive problem

$$\begin{cases} \operatorname{div}(\mu \nabla v_j) - \kappa^2 v_j = 0 & \text{in } \Omega_j^h, \\ v_j = p_j & \text{on } \Gamma_j^h. \end{cases}$$

In practice, the local solutions v_j can be computed in parallel using the same numerical scheme and mesh as for the solutions u_j .

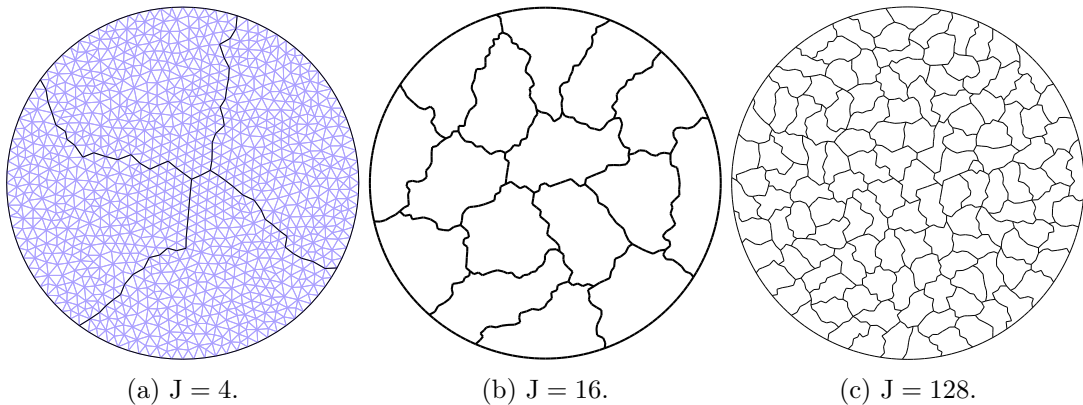


Figure 3: Examples of mesh partitions.

The research code that was used to run the tests was developed specifically to test the method and uses \mathbb{P}_1 -Lagrange finite elements. It is written in JULIA [3] and was validated on standard scattering test cases. The meshes are generated by GMSH [24] and partitioned using METIS [26] through the JULIA API. The integral operator matrices are computed thanks to the BEMTOOL library ², written in C++. The tests were performed on a 8-cores *Intel XEON W-2145* at 3.7 GHz equipped with 256 Go of RAM.

11.1 Influence of typical mesh size

We present a first test case consisting of a disk of radius $R = 1$ split roughly (using a mesh partitioner) in four quarters, see Figure 3a. The interest of this test case is the presence of pure interior junction points where three domains share a common vertex.

²<https://github.com/xclaeys/BemTool>

The full convergence history of the relative \mathbb{H}^1 error (32) for the Richardson and GMRES algorithms are provided for this test case in Figure 4 as an illustrative example of typical convergence.

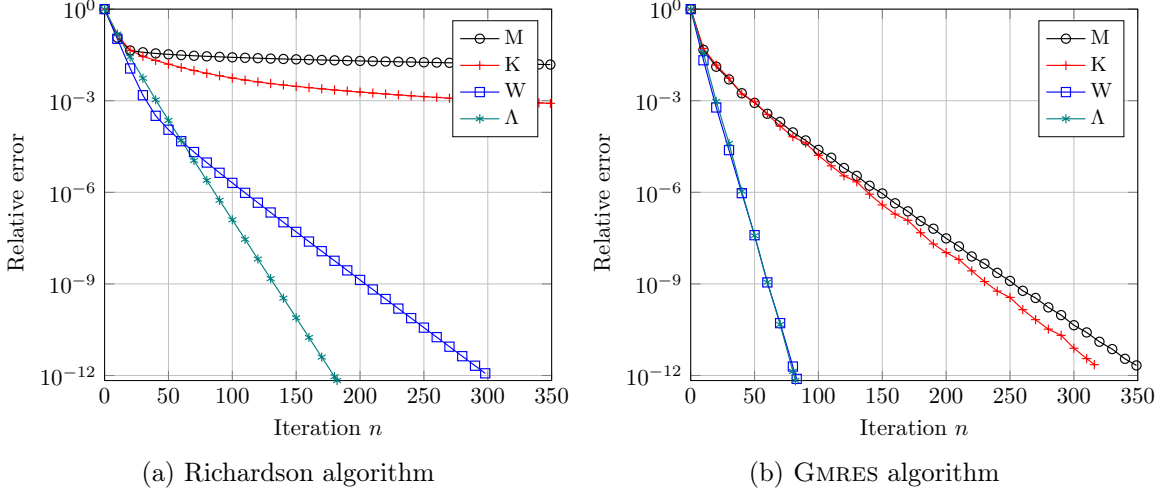


Figure 4: An example of convergence history. Fixed parameters $\kappa = 5$, $J = 4$, $N_\lambda = 40$, 2D, disk of radius $R = 1$.

We report the number of iterations to reach convergence with respect to mesh refinement in Figure 5 for the Richardson and GMRES algorithms. The refinement of the mesh is indicated by the number of points per wavelength N_λ which is inversely proportional to the typical mesh size. In Figure 5b we also report the number of GMRES iterations that are required to achieve the same error to solve the full (undecomposed) linear system (line plot labelled ‘No DDM’). We see that this iteration count has a growth which is approximately quadratic with respect to N_λ , illustrating the deterioration of the matrix conditioning as the mesh is refined.

For the local operators M and K the convergence is not uniform with respect to mesh refinement and a large number of iterations is required to get to the set tolerance. The growth of the iteration count appears to be quasi quadratic with respect to N_λ for the Richardson algorithm and quasi linear for the GMRES algorithm. For small mesh size the convergence may not even be reached within 10^5 iterations. In contrast, the non-local operators W and Λ exhibit uniform convergence in all cases, with a very moderate number of iterations required to reach the set tolerance.

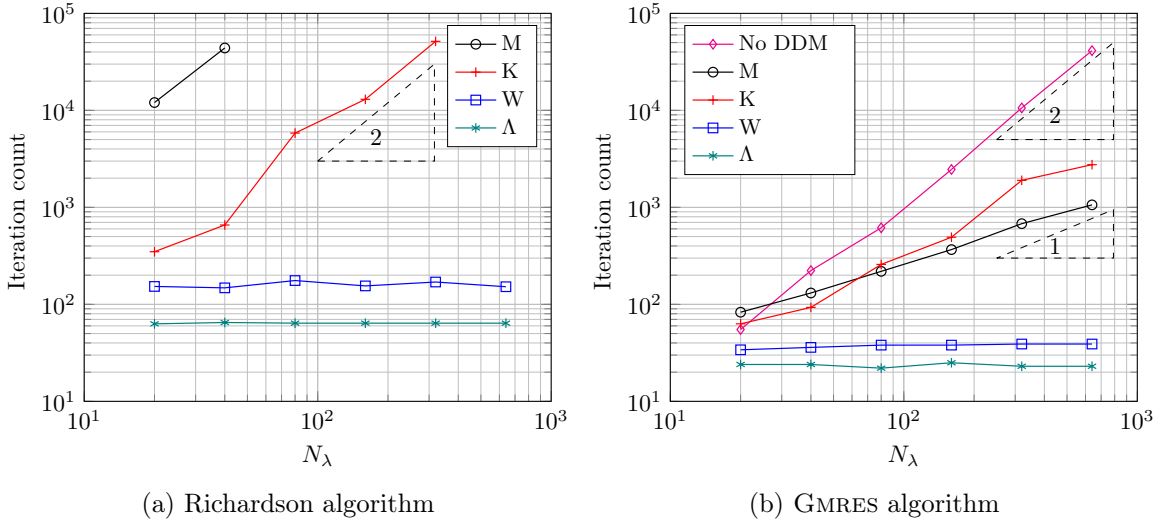


Figure 5: Number of iterations with respect to the number of mesh points per wavelength N_λ . Fixed parameters $\kappa = 1$, $J = 4$, 2D, disk of radius $R = 1$.

We also provide some numerical results obtained in 3D. The domain Ω is now a ball of radius $R = 1$ partitioned into eight subdomains, which generate interior junction curves where three domains share common edges. Figure 6 reports the iteration count with respect to mesh refinement. Again in this case, we clearly identify the non-uniformity of the convergence for the local operators M and K while the non-local operators W and Λ exhibit h -uniform convergence.

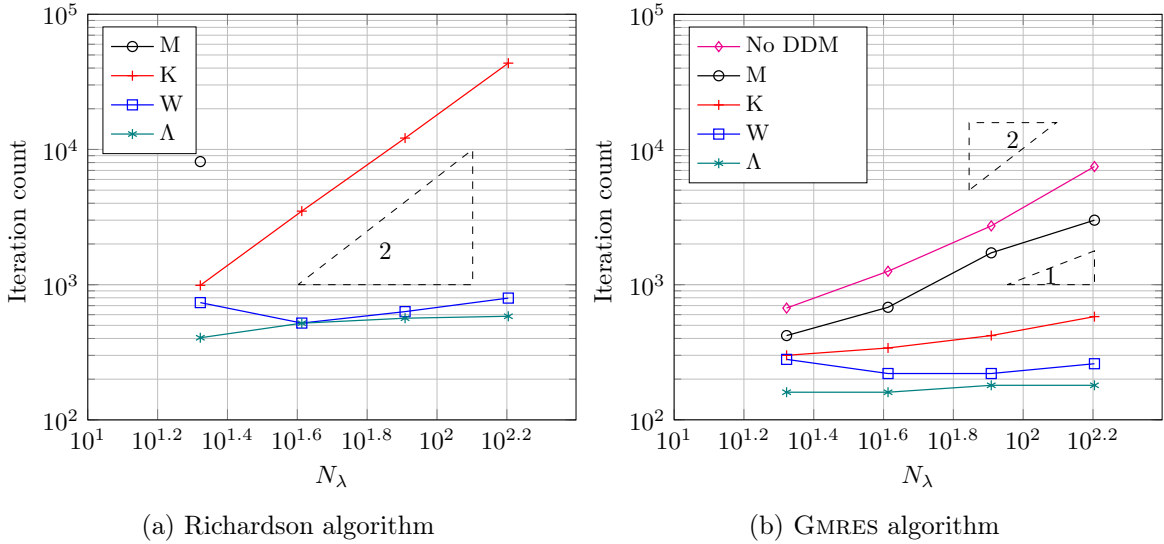


Figure 6: Number of iterations with respect to the number of mesh points per wavelength N_λ . Fixed parameters $\kappa = 1$, $J = 8$, 3D, sphere of radius $R = 1$. GMRES algorithm.

11.2 Influence of the wavenumber

For the two-dimensional case, we now report the dependency of the iteration count with respect to the wavenumber κ , see Figure 7. As the wavenumber κ increases, the discrete (as well as the continuous) problem gets harder. This is indicated again by the increase in the iteration count of the GMRES algorithm for the undecomposed problem (line plot labelled ‘No DDM’ in Figure 7b). For this case, the growth is linear with respect to κ . In contrast, for all the impedance operators under study, we notice a sub-linear growth of the number of iteration with respect to κ . The iteration count is especially moderate for the non-local operators.

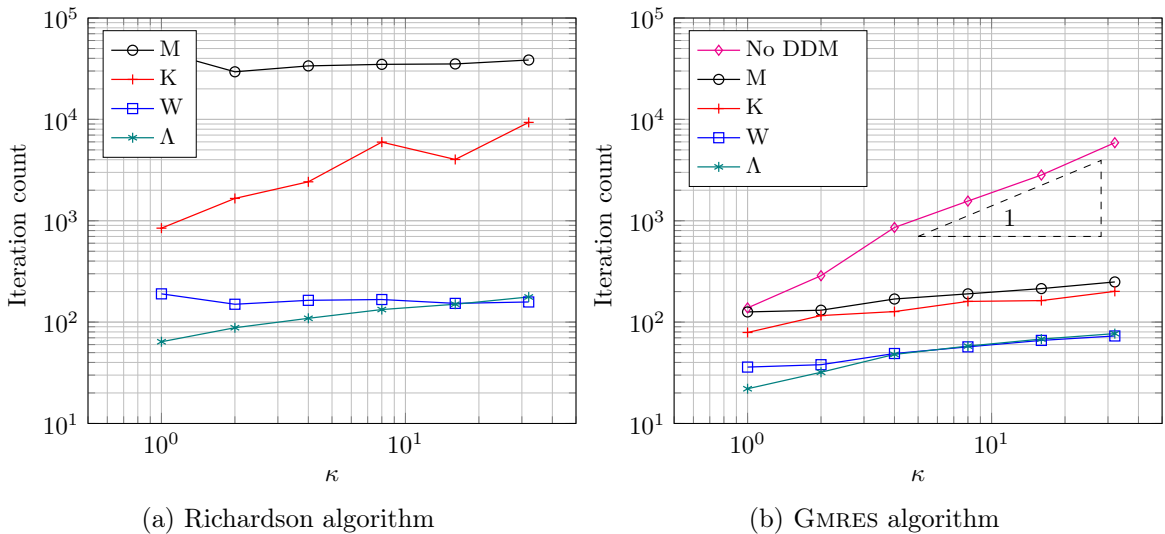


Figure 7: Number of iterations with respect to the wavenumber κ . Fixed parameters $J = 4$, $N_\lambda = 30$, 2D, disk of radius $R = 1$.

11.3 Scalability of the method

We finally study the dependency of the method with respect to the number of subdomains J of the mesh partition.

We start with a strong scaling test in 2D. Figure 8 reports the iteration count with respect to J varying from 2 to 1024 subdomains. One can notice a sub-linear increase in the number of iterations to get to a converged solution. Notice that in this case the undecomposed linear system is kept the same. Hence, the fact that the discrete problem gets harder is a pure artificial effect of the DDM. Interestingly, we see that the number of iterations levels out for the coercive DtN operator, in a regime where the size of the sub-problems gets really small compared to the wavelength of the problem.

A weak scaling test was also performed, this time with a domain increasing in size as the number of sub-domains J grows. Figure 9 reports the iteration count with respect to J for the 2D and 3D cases. The size of the domain is chosen to grow like $J^{1/d}$ where d is the dimension of ambient space, so as to keep a fixed size (in terms of DOFs) for the local subdomains. In 2D the domain is a disk of radius increasing from $R = 1$ to $R = 16$, and in 3D the domain is

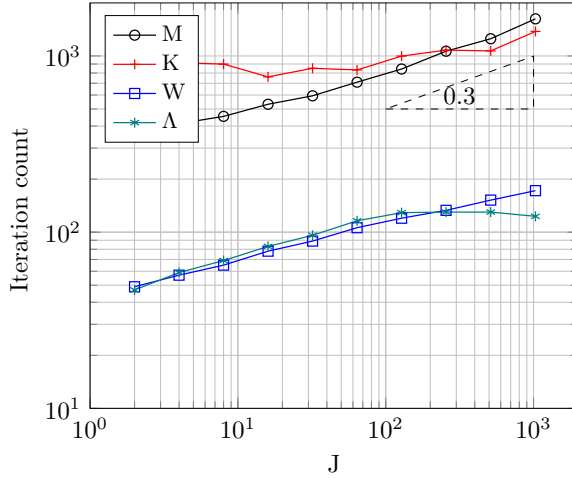
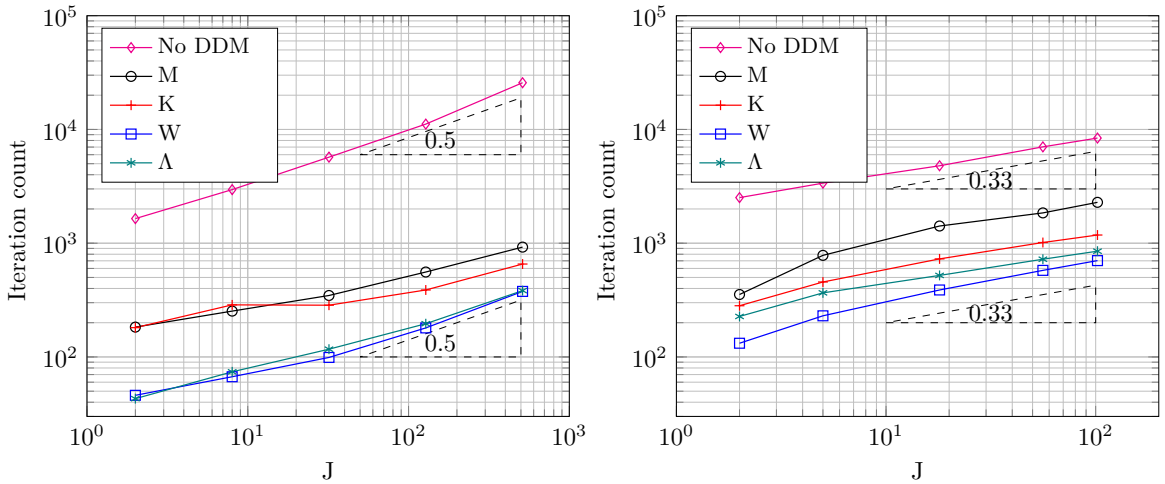


Figure 8: Number of iterations with respect to the number of subdomains J (Strong scaling). Fixed parameters $\kappa = 2$, $N_\lambda = 100$, 2D, disk of radius $R = 4$. GMRES algorithm.

a sphere of radius increasing from $R = 1$ to $R = 3.7$. The growth of the number of iteration to reach the set tolerance also appears to scale like $J^{1/d}$.



(a) Fixed parameters $\kappa = 5$, $N_\lambda = 40$, 2D

(b) Fixed parameters $\kappa = 2$, $N_\lambda = 30$, 3D

Figure 9: Number of iterations with respect to the number of subdomains J (Weak scaling). Disk (left) and sphere (right) of increasing radius. GMRES algorithm.

11.4 Heterogeneous medium

We close the numerical experiment section with some results in heterogeneous medium in 2D. The domain of propagation Ω is still a disk of radius $R = 1$, but this time with a circular inclusion of a different medium in the region with radius $R \leq 0.5$. The coefficient μ is still equal to 1 outside the inclusion and takes the value $\mu = 1 + \mu_r$ inside, with μ_r varying from 0 (homogeneous medium) to 4. Figure 10 reports the iteration counts for the GMRES algorithm

as the medium varies. The partition is composed of 10 sub-domains so that some interfaces are cut by the discontinuity in the medium. One can observe that the number of iterations to get to convergence increases greatly for the undecomposed problem (line plot labelled ‘No DDM’). This is due to the apparition in the solution of quasi “modes” of the inclusion with large amplitude. For an illustration of this effect, the modulus of the total field is represented in Figure 11 for the value $\mu_r = 4$. On the other hand, the DD algorithm performs well, with a number of iterations only mildly growing.

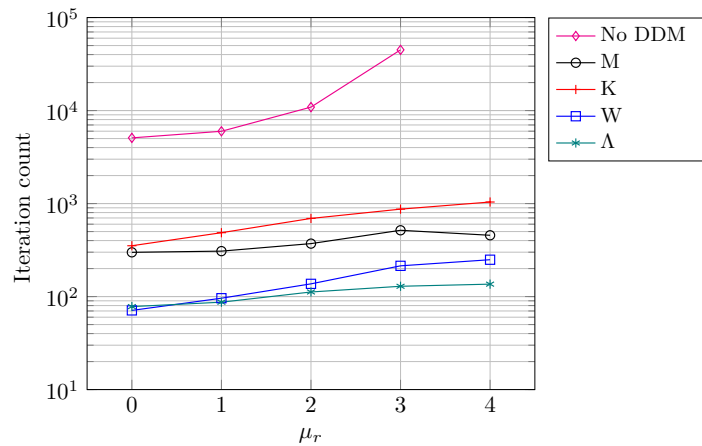


Figure 10: Number of iterations with respect to increasing contrast in μ . Fixed parameters $\kappa = 10$, $J = 10$, $N_\lambda = 50$, 2D, disk of radius $R = 1$. GMRES algorithm.

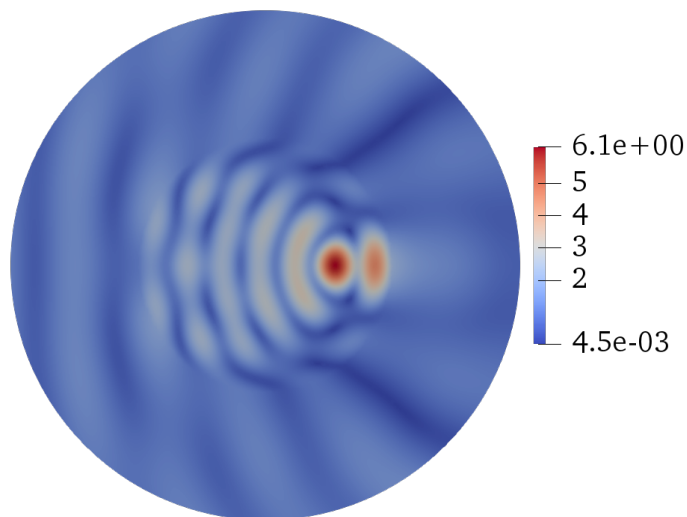


Figure 11: Modulus of the total field. Fixed parameters $\kappa = 10$, $N_\lambda = 50$, 2D, disk of radius $R = 1$, $\mu_r = 4$.

Acknowledgements

This work was supported by the project NonlocalDD funded by the French National Research Agency, grant ANR-15-CE23-0017-01. The authors would like to thank Patrick Joly and Francis Collino for many inspiring discussions and, in particular, for pointing a simplification in the proof of Corollary 5.3.

References

- [1] A. Bendali and Y. Boubendir. Dealing with cross-points in a non-overlapping domain decomposition solution of the helmholtz equation. In G. Cohen, P. Joly, E. Heikkola, and P. Neittaanmäki, editors, *Mathematical and Numerical Aspects of Wave Propagation WAVES 2003: Proceedings of The Sixth International Conference on Mathematical and Numerical Aspects of Wave Propagation*, pages 319–324, 2003.
- [2] A. Bendali and Y. Boubendir. Non-overlapping domain decomposition method for a nodal finite element method. *Numerische Mathematik*, 103(4):515–537, Jun 2006.
- [3] J. Bezanson, A. Edelman, S. Karpinski, and V.B. Shah. Julia: A fresh approach to numerical computing. *SIAM review*, 59(1):65–98, 2017.
- [4] Y. Boubendir, X. Antoine, and C. Geuzaine. A Quasi-Optimal Non-Overlapping Domain Decomposition Algorithm for the Helmholtz Equation. *J. Comp. Phys.*, 213(2):262–280, 2012.
- [5] S.C. Brenner and L.R. Scott. *The mathematical theory of finite element methods*. 3rd ed., volume 15. New York, NY: Springer, 3rd ed. edition, 2008.
- [6] X. Claeys. A single trace integral formulation of the second kind for acoustic scattering. Technical Report 14, Seminar for Applied Mathematics, ETH Zürich, Switzerland, 2011.
- [7] X. Claeys. Quasi-local multitrace boundary integral formulations. *Numer. Methods Partial Differential Equations*, 31(6):2043–2062, 2015.
- [8] X. Claeys. A new variant of the optimised schwarz method for arbitrary non-overlapping subdomain partitions, 2019.
- [9] X. Claeys, F. Collino, P. Joly, and E. Parolin. A discrete domain decomposition method for acoustics with uniform exponential rate of convergence using non-local impedance operators. In *Domain Decomposition Methods in Science and Engineering XXV*. Springer International Publishing, 2019.
- [10] X. Claeys and R. Hiptmair. Multi-trace boundary integral formulation for acoustic scattering by composite structures. *Comm. Pure Appl. Math.*, 66(8):1163–1201, 2013.
- [11] X. Claeys, B. Thierry, and F. Collino. Integral equation based optimized Schwarz method for electromagnetics. In *Domain decomposition methods in science and engineering XXIV*, volume 125 of *Lect. Notes Comput. Sci. Eng.*, pages 187–194. Springer, Cham, 2018.

- [12] F. Collino, S. Ghanemi, and P. Joly. Domain decomposition method for harmonic wave propagation: a general presentation. *Computer Methods in Applied Mechanics and Engineering*, 184(2):171 – 211, 2000.
- [13] F. Collino, P. Joly, and M. Lecouvez. Exponentially convergent non overlapping domain decomposition methods for the helmholtz equation. *ESAIM M2AN*, 2019. accepted.
- [14] B. Després. Décomposition de domaine et problème de Helmholtz. *C. R. Acad. Sci. Paris Sér. I Math.*, 311(6):313–316, 1990.
- [15] B. Després. Domain decomposition method and the Helmholtz problem. In *Mathematical and numerical aspects of wave propagation phenomena (Strasbourg, 1991)*, pages 44–52. SIAM, Philadelphia, PA, 1991.
- [16] B. Després. *Méthodes de décomposition de domaine pour les problèmes de propagation d’ondes en régime harmonique. Le théorème de Borg pour l’équation de Hill vectorielle*. Institut National de Recherche en Informatique et en Automatique (INRIA), Rocquencourt, 1991. Thèse, Université de Paris IX (Dauphine), Paris, 1991.
- [17] B. Després. Domain decomposition method and the Helmholtz problem. II. In *Second International Conference on Mathematical and Numerical Aspects of Wave Propagation (Newark, DE, 1993)*, pages 197–206. SIAM, Philadelphia, PA, 1993.
- [18] V. Dolean, P. Jolivet, and F. Nataf. *An introduction to domain decomposition methods*. Society for Industrial and Applied Mathematics (SIAM), Philadelphia, PA, 2015. Algorithms, theory, and parallel implementation.
- [19] M. El Bouajaji, B. Thierry, X. Antoine, and C. Geuzaine. A quasi-optimal domain decomposition algorithm for the time-harmonic maxwell’s equations. *Journal of Computational Physics*, 294:38–57, 2015.
- [20] M. Gander and F. Kwok. On the applicability of Lions’ energy estimates in the analysis of discrete optimized schwarz methods with cross points. *Lecture Notes in Computational Science and Engineering*, 91, 01 2013.
- [21] M.J. Gander, F. Magoulès, and F. Nataf. Optimized Schwarz methods without overlap for the Helmholtz equation. *SIAM J. Sci. Comput.*, 24(1):38–60, 2002.
- [22] M.J. Gander and K. Santugini. Cross-points in domain decomposition methods with a finite element discretization. *Electron. Trans. Numer. Anal.*, 45:219–240, 2016.
- [23] M.J. Gander and Y. Xu. Optimized Schwarz methods for model problems with continuously variable coefficients. *SIAM J. Sci. Comput.*, 38(5):A2964–A2986, 2016.
- [24] C. Geuzaine and J.-F. Remacle. Gmsh: A 3-d finite element mesh generator with built-in pre- and post-processing facilities. *International Journal for Numerical Methods in Engineering*, 79:1309 – 1331, 09 2009.
- [25] F. Ihlenburg. *Finite element analysis of acoustic scattering*, volume 132 of *Applied Mathematical Sciences*. Springer-Verlag, New York, 1998.

- [26] G. Karypis and V. Kumar. A fast and high quality schema for partitioning irregular graphs. *Siam Journal on Scientific Computing*, 20, 01 1999.
- [27] M. Lecouvez. *Iterative methods for domain decomposition without overlap with exponential convergence for the Helmholtz equation*. Theses, Ecole Polytechnique, July 2015.
- [28] S. Loisel. Condition number estimates for the nonoverlapping optimized schwarz method and the 2-lagrange multiplier method for general domains and cross points. *SIAM Journal on Numerical Analysis*, 51(6):3062–3083, 2013.
- [29] F. Magoulès, P. Iványi, and B. H. V. Topping. Non-overlapping Schwarz methods with optimized transmission conditions for the Helmholtz equation. *Comput. Methods Appl. Mech. Engrg.*, 193(45–47):4797–4818, 2004.
- [30] A. Modave, A. Royer, X. Antoine, and C. Geuzaine. An optimized Schwarz domain decomposition method with cross-point treatment for time-harmonic acoustic scattering. working paper or preprint, January 2020.
- [31] C. Pechstein. *Finite and boundary element tearing and interconnecting solvers for multiscale problems*, volume 90 of *Lecture Notes in Computational Science and Engineering*. Springer, Heidelberg, 2013.
- [32] S.A. Sauter and C. Schwab. *Boundary element methods*, volume 39 of *Springer Series in Computational Mathematics*. Springer-Verlag, Berlin, 2011. Translated and expanded from the 2004 German original.
- [33] L.R. Scott and S. Zhang. Finite element interpolation of nonsmooth functions satisfying boundary conditions. *Math. Comput.*, 54(190):483–493, 1990.
- [34] A. St-Cyr, D. Rosenberg, and Sang D. Kim. Optimized schwarz preconditioning for sem based magnetohydrodynamics. In Michel Bercovier, Martin J. Gander, Ralf Kornhuber, and Olof Widlund, editors, *Domain Decomposition Methods in Science and Engineering XVIII*, pages 209–216, 2009.
- [35] O. Steinbach. *Numerical approximation methods for elliptic boundary value problems*. Springer, New York, 2008. Finite and boundary elements, Translated from the 2003 German original.
- [36] A. Toselli and O. Widlund. *Domain decomposition methods—algorithms and theory*, volume 34 of *Springer Series in Computational Mathematics*. Springer-Verlag, Berlin, 2005.